

AC OPF in Radial Distribution Networks - Part I: On the Limits of the Branch Flow Convexification and the Alternating Direction Method of Multipliers

Konstantina Christakou^{a,b}, Dan-Cristian Tomozei^c, Jean-Yves Le Boudec^a,
Mario Paolone^{b,*}

^a*Laboratory for Communications and Applications 2, Ecole Polytechnique Fédérale de
Lausanne, CH-1015 Lausanne, Switzerland*

^b*Distributed Electrical Systems Laboratory, Ecole Polytechnique Fédérale de Lausanne,
CH-1015 Lausanne, Switzerland*

^c*Cisco Systems, Inc, EPFL Innovation Park Building E 1015 Lausanne, Switzerland*

Abstract

The optimal power-flow problem (OPF) has always played a key role in the planning and operation of power systems. Due to the non-linear nature of the AC power-flow equations, the OPF problem is known to be non-convex, therefore hard to solve. Most proposed methods for solving the OPF rely on approximations (e.g., of the network model) that render the problem convex, but that consequently yield inexact solutions. Recently, Farivar and Low proposed in [1, 2] a method that is claimed to be exact for the case of radial distribution systems under specific assumptions, despite no apparent approximations. In our work, we show that it is, in fact, not exact. On one hand, there is a misinterpretation of the physical network model related to the ampacity constraint of the lines' current flows and, on the other hand, the proof of the exactness of the proposed relaxation requires unrealistic assumptions related to the unboundedness of specific control variables. We also show that the extension of this approach to account for exact line models might provide physically infeasible solutions. Therefore, there is a need to develop algorithms for the solution of the

*Corresponding author. Phone number: +41 21 69 32662, Postal address: EPFL STI IEL
DESL ELL 136 (Bâtiment ELL), Station 11, CH-1015 Lausanne

Email addresses: konstantina.christakou@epfl.ch (Konstantina Christakou),
dtomozei@cisco.com (Dan-Cristian Tomozei), jean-yves.leboudec@epfl.ch (Jean-Yves Le
Boudec), mario.paolone@epfl.ch (Mario Paolone)

non-approximated OPF problem that remains inherently non-convex. Recently, several contributions have proposed OPF algorithms that rely on the use of the alternating-direction method of multipliers (ADMM). However, as we show in this work, there are cases for which the ADMM-based solution of the non-relaxed OPF problem fails to converge. To overcome the aforementioned limitations, we propose a specific algorithm for the solution of a non-approximated, non-convex OPF problem in radial distribution systems. In view of the complexity of the contribution, this work is divided in two parts. In this first part, we specifically discuss the limitations of both BFM and ADMM to solve the OPF problem.

Keywords: OPF, ADMM, decomposition methods, method of multipliers, convex relaxation, active distribution networks.

1. Introduction

The category of optimal power-flow problems (OPFs) represents the main set of problems for the optimal operation of power systems. The first formulation of an OPF problem appeared in the early 1960s and has been well-defined ever since [3]. It consists in determining the operating point of controllable resources in an electric network in order to satisfy a specific network objective subject to a wide range of constraints. Typical controllable resources considered in the literature are generators, storage systems, on-load tap changers (OLTC), flexible AC transmission systems (FACTS) and loads (e.g., [4, 5, 6, 7, 8]). The network objective is usually the minimization of losses or generation costs, and typical constraints include power-flow equations, capability curves of the controllable resources, as well as operational limits on the line power-flows and node voltages (e.g., [9]).

The OPF problem is known to be non-convex, thus difficult to solve efficiently (e.g., [10, 11, 12]). Since the problem was first formulated, several techniques have been used for its solution. Among others, non-linear and quadratic programming techniques, Newton-based methods, interior point methods in the earlier years, as well as heuristic approaches based on genetic algorithms,

evolutionary programming, and particle-swarm optimization in recent years
20 (e.g., [13, 14, 15]).

Currently, the OPF problem is becoming more compelling due to the increasing penetration of embedded generation in distribution networks, essentially composed by renewable resources. The distributed nature of such resources, as well as their large number and potential stochasticity increase significantly the
25 complexity of the OPF problem and bring about the need for distributed solutions. In this direction, several distributed algorithms have been proposed in the literature. In [16, 17] the authors design a dual-ascent algorithm for optimal reactive power-flow with power and voltage constraints. In [18, 19] dual decomposition is used as the basis for the distributed solution of the OPF problem.
30 Finally, a significant number of contributions propose distributed formulations of the OPF problem that are based on the alternating direction method of multipliers (ADMM) (e.g., [20, 18, 21, 22, 23, 24]).

However, due to the non-convex nature of the problem, most of the proposed schemes either do not guarantee to yield an optimal solution or they are based on
35 approximations that convexify the problem in order to guarantee convergence. These approximations, often, either lead to (i) misinterpretation of the system model [25] or (ii) solutions that, even though mathematically sound, might be far away from the real optimal solution, thus having little meaning for the grid operation [26].

40 Recently, Farivar and Low proposed in [1, 2] a convexification of the problem that is claimed to be exact for radial networks. In Part I of this paper, we show that this claim is not exact, as the convexification of the problem leads to an inexact system model. We also show that the method of ADMM-based decomposition, which comes together with the convexification, does not work for a
45 correct system model. As an alternative, we propose in Part II an algorithm for the solution of the correct AC OPF problem in radial networks. Like ADMM, it uses an augmented Lagrangian, but unlike ADMM, it uses primal decomposition [27] and does not require that the problem be convex. We consider a direct-sequence representation of the electric distribution grid and we present

50 both a centralized and a decentralized asynchronous version of the algorithm.

The structure of this first part is as follows. In Section 2 we present the generic formulation of the OPF problem in radial distribution systems and we classify several OPF algorithms based on the approximations and assumptions on which they rely. In Section 3 we discuss the limitations and applicability of
 55 the Farivar-Low formulation of the OPF problem proposed in [1, 2]. We provide, in Section 4, the ADMM-based solution of the original non-approximated OPF problem. In the same section, we highlight specific cases where the ADMM-based algorithm fails to converge. Finally, we provide the main observations and concluding remarks for this part in Section 4.2.

60 2. Generic Formulation of the OPF Problem

In the rest of the paper, we consider a balanced radial network composed of buses (\mathcal{B}), lines (\mathcal{L}), generators (\mathcal{G}) and loads (\mathcal{C}). The network admittance matrix is denoted by Y . Several generators/loads can be connected to a bus $b \in \mathcal{B}$. We denote that a generator $g \in \mathcal{G}$ or a load $c \in \mathcal{C}$ is connected to a bus by
 65 “ $g \in b$ ” and “ $c \in b$ ”. A line $\ell \in \mathcal{L}$ is represented using a π -equivalent model and it has a receiving and a sending end denoted by ℓ^+ and ℓ^- . Each line is connected to two adjacent buses: $\beta(\ell^+)$ and $\beta(\ell^-)$, respectively.

2.1. Generic OPF Formulation

The traditional formulation of the OPF problem consists in minimizing a specific network objective:

$$\min_{\bar{S}_g, \bar{S}_c, \bar{S}_\ell^+, \bar{S}_\ell^-, \bar{I}_\ell^+, \bar{I}_\ell^-, \bar{V}_b} \sum_{g \in \mathcal{G}} C_g(\bar{S}_g) + \sum_{c \in \mathcal{C}} C_c(\bar{S}_c) \quad (1)$$

The first term of the network objective (C_g) in (1) is typically a non-decreasing
 70 convex function accounting for the minimization of the generation costs or the network real power losses. The second term (C_c) is included in the objective when the cost of non-supplied load is taken into account.

The following set of constraints is considered¹:

$$\sum_{g \in b} \bar{S}_g - \sum_{c \in b} \bar{S}_c + \sum_{\beta(\ell^+) = b} \bar{S}_{\ell^+} + \sum_{\beta(\ell^-) = b} \bar{S}_{\ell^-} = 0, \quad \forall b \in \mathcal{B} \quad (2)$$

$$\bar{S}_{\ell^+} = \bar{V}_{\beta(\ell^+)} \underline{I}_{\ell^+}, \quad \bar{S}_{\ell^-} = \bar{V}_{\beta(\ell^-)} \underline{I}_{\ell^-}, \quad \forall \ell \in \mathcal{L} \quad (3)$$

$$\bar{I}_{\ell^+} = \bar{Y}_{\ell} (\bar{V}_{\beta(\ell^+)} - \bar{V}_{\beta(\ell^-)}) + \bar{Y}_{\ell_0^+} \bar{V}_{\beta(\ell^+)}, \quad \forall \ell \in \mathcal{L} \quad (4)$$

$$\bar{I}_{\ell^-} = \bar{Y}_{\ell} (\bar{V}_{\beta(\ell^-)} - \bar{V}_{\beta(\ell^+)}) + \bar{Y}_{\ell_0^-} \bar{V}_{\beta(\ell^-)}, \quad \forall \ell \in \mathcal{L} \quad (5)$$

$$V_{min} \leq |\bar{V}_b| \leq V_{max}, \quad \forall b \in \mathcal{B} \quad (6)$$

$$|\bar{S}_{\ell^+}| \leq S_{\ell_{max}}, \quad \text{or} \quad |\bar{I}_{\ell^+}| \leq I_{\ell_{max}}, \quad \forall \ell \in \mathcal{L} \quad (7)$$

$$|\bar{S}_{\ell^-}| \leq S_{\ell_{max}}, \quad \text{or} \quad |\bar{I}_{\ell^-}| \leq I_{\ell_{max}}, \quad \forall \ell \in \mathcal{L} \quad (8)$$

$$\bar{S}_g \in \mathcal{H}_g, \quad \forall g \in \mathcal{G} \quad \text{and} \quad \bar{S}_c \in \mathcal{H}_c, \quad \forall c \in \mathcal{C} \quad (9)$$

where, \bar{S} denotes the complex power², \bar{V}_b is the direct sequence phase-to-ground
75 voltage of node b , \bar{I}_{ℓ^+} (\bar{I}_{ℓ^-}) is the current flow in the receiving (sending) end of
line ℓ , \bar{Y}_{ℓ} is the longitudinal admittance of a line, $\bar{Y}_{\ell_0^+}$ ($\bar{Y}_{\ell_0^-}$) is the shunt capac-
itance at the receiving (sending) end of the line, and $\mathcal{H}_g, \mathcal{H}_c$ are the capability
curve of the generator g and the limits of the load c respectively³. If a generator
(load) is non-controllable then the set \mathcal{H}_g (\mathcal{H}_c) is limited to a single point.

80 The first constraint (2) corresponds to the power balance constraint at each
network bus, whereas (3) is an alternative way to define the AC power flow
equations. Constraints (6) and (7) are so-called node voltage and lines ampac-
ity constraints, i.e., limits on node voltages and line power/current flows. The
last constraints (9) represent the capability limits that each of the controllable
85 devices should respect.

The equality constraints (3) render the OPF problem non-convex and, there-

¹In the rest of the paper, complex numbers are denoted with a bar above (e.g., \bar{V}) and complex conjugates with a bar below (e.g., \underline{V}).

²We use the convention that positive values represent power injection and negative power consumption.

³Note that different types of controllable generators or loads can be accounted for via their corresponding capability curves/limits.

fore, difficult to solve efficiently. The majority of the proposed algorithms in the literature rely on several approximations and/or convex relaxations and seek a solution to a modified OPF problem. In what follows, we describe and discuss
90 the most common approximations.

2.2. Approximations of the OPF Problem

In general, the approximations used in the formulation of an OPF problem can be categorized in two large groups: approximations of the physical network models and methods that relax the space of the solutions and/or control
95 variables.

In the first case, we can find OPF formulations that rely mainly on linearizations of the AC power flow equations. Such attempts typically (i) consider the DC power flow, (ii) use the decoupled AC power flow or (iii) neglect the network losses and/or the transverse parameters of the lines. Specifically, the concepts
100 of the DC and the decoupled OPF have been extensively used in the literature (e.g., [28, 29, 30, 31]), as they approximate the OPF problem with linear programming problems and, therefore, enable its fast resolution. Furthermore, the authors in [22] use the so-called Dist-Flow equations ([32]) to linearize the power flows and propose an ADMM-based OPF algorithm that neglects the real and
105 reactive losses. Finally, several contributions rely on simplified network line-models that neglect the transverse parameters, resulting in inaccuracies of the physical system model (e.g., [33, 34, 35]).

In the second case, we can find OPF formulations where, typically, the constraints are relaxed in order to convexify the problem. In particular, a large number of contributions recently proposed a SDP formulation of the OPF problem,
110 where the rank-one constraint of a matrix is relaxed and the algorithm is claimed to yield zero-duality gap for radial distribution networks (e.g., [36, 18, 19]). Another relaxation is proposed in [35] where the OPF problem is cast as a second order cone programming. A similar technique is used in [37], where the equality
115 constraints of the branch flows are relaxed.

In both the aforementioned categories of approximations, the modified OPF

formulations guarantee convergence of the proposed algorithms. The reached solutions, however, even though mathematically sound, are not always meaningful for the grid operation. The DC and the decoupled OPF work sufficiently well for transmission systems, nevertheless they can introduce large errors when used for solving the OPF in the case of distribution systems (e.g., [38]). As far as the semidefinite relaxation is concerned, its limitations have been recently investigated. The authors in [26] show through practical examples, that in the case of negative locational marginal prices or strict line-flow constraints it can lead to solutions that are not valid, namely for which the duality gap is not zero. Furthermore, in [39] the authors show the existence of multiple local optima of the OPF problem due to the feasible region being disconnected and due to the nonlinearities of the constraints; they show that the SDP formulation of the OPF problem fails to find the global optimum in cases where there are multiple local optima. In the same direction, a recent review ([34]) summarizes the semidefinite relaxations applied to the OPF problem and discusses their limitations.

Recently, another formulation of the OPF problem has been proposed ([40, 41, 1, 2, 42]). This formulation also belongs to the category of the semidefinite relaxations and uses the so-called branch-flow model (BFM) for describing the network. The BFM essentially describes the network flows by using as variables the currents and the powers of the various network branches, instead of the nodal injections. In [1, 2] Farivar and Low propose an OPF formulation that relies on the BFM representation of the network and they present a two-step relaxation procedure that turns the problem into a second-order cone program (SOCP). The authors prove that under specific assumptions both relaxation steps are exact for the case of radial networks, hence a globally optimal OPF solution can be retrieved by solving the relaxed convex problem.

In what follows, we first briefly recall the Farivar-Low formulation of the OPF problem and then we investigate the applicability of the branch flow model to the OPF formulation. We show, on one hand, that the Farivar-Low model misinterprets the physical network model by imposing an ampacity constraint on

a fictitious line-current flow that neglects the contribution of the shunt components of the line and that, on the other hand, the proof of the exactness of the proposed relaxation requires unrealistic assumptions related to the unboundedness of specific control variables.

3. On the Limits of the Farivar-Low Approach for the Solution of the OPF Problem

3.1. The Farivar-Low Formulation of the OPF Problem

We assume the same objective function as in Eq. 1 and again consider that the network lines are represented using a π -model. Contrary to the formulation in (2)-(9), we reformulate the constraints of the OPF problem by using the branch power and current flows as variables, similarly to [1]. To this end, we denote by \bar{S}_ℓ and \bar{I}_ℓ the power and the current that flow across the longitudinal elements of a network line ℓ from the receiving toward the sending end, for which it holds that

$$\bar{I}_\ell = \bar{Y}_\ell(\bar{V}_{\beta(\ell^+)} - \bar{V}_{\beta(\ell^-)}), \quad \forall \ell \in \mathcal{L} \quad (10)$$

$$\bar{S}_\ell = \bar{V}_{\beta(\ell^+)} \bar{I}_\ell, \quad \forall \ell \in \mathcal{L} \quad (11)$$

The power and current flows along the shunt elements of the lines are taken into account in the bus power balance constraints as nodal injections. In this direction, we denote by \bar{Y}_{b_0} the sum of all the shunt elements of the lines that are adjacent to bus b . Hence, the constraints of the OPF problem are reformulated as follows by Farivar and Low:

$$\sum_{g \in b} \bar{S}_g - \sum_{c \in b} \bar{S}_c = \sum_{\beta(\ell^+)=b} \bar{S}_\ell - \sum_{\beta(\ell^-)=b} (\bar{S}_\ell - \bar{Y}_\ell^{-1} |\bar{I}_\ell|^2) - \bar{Y}_{b_0} |\bar{V}_b|^2, \quad \forall b \in \mathcal{B} \quad (12)$$

$$|\bar{I}_\ell|^2 = \frac{|\bar{S}_\ell|^2}{|\bar{V}_{\beta(\ell^+)}|^2}, \quad \forall \ell \in \mathcal{L} \quad (13)$$

$$|\bar{V}_{\beta(\ell^-)}|^2 = |\bar{V}_{\beta(\ell^+)}|^2 + |\bar{Y}_\ell^{-1}|^2 |\bar{I}_\ell|^2 - (\bar{Y}_\ell^{-1} \bar{S}_\ell + \bar{Y}_\ell^{-1} \bar{S}_\ell), \quad \forall \ell \in \mathcal{L} \quad (14)$$

$$V_{min}^2 \leq |\bar{V}_b|^2 \leq V_{max}^2, \quad \forall b \in \mathcal{B} \quad (15)$$

$$|\bar{I}_\ell|^2 \leq I_{\ell_{max}}^2, \forall \ell \in \mathcal{L} \quad (16)$$

$$Re(\bar{S}_g) \in [P_{gmin}, P_{gmax}], Im(\bar{S}_g) \in [Q_{gmin}, Q_{gmax}], \forall g \in \mathcal{G} \quad (17)$$

$$Re(\bar{S}_c) \in [P_{cmin}, P_{cmax}], Im(\bar{S}_c) \in [Q_{cmin}, Q_{cmax}], \forall c \in \mathcal{C} \quad (18)$$

160 Note that in the Farivar-Low formulation of the OPF problem, the capability curves of the controllable loads and generators, i.e., constraints (17,18) on the nodal power \bar{S} are limited to rectangular regions. This is essential for the conic relaxation proposed in [1, 2].

Starting from this formulation, Farivar and Low relax the equality constraints in (13) to inequalities and cast the aforementioned problem as a second-
165 order cone program. They also prove that for radial networks a global solution of the original OPF problem can be recovered from the solution of the relaxed problem if there are no upper bounds on the loads. In other words, Farivar and Low solve (12)-(18) by setting $P_{cmax} = \infty$ and $Q_{cmax} = \infty$ in constraint (18).

170 We show, in what follows, that this formulation is not equivalent to (1-9). In particular, constraint (16) (constraint (9) in [1]) is only an approximation of the ampacity constraints and, moreover, the assumptions on the controllability and bounds of the energy resources in the network are unrealistic.

3.2. Misinterpretation of the Physical Network Model in the Farivar-Low OPF 175 Formulation

The branch-flow model has been often used in load-flow studies (e.g., [43, 44]) and constitutes an accurate representation of the network model. The first problem with the Farivar-Low formulation in (12)-(18) is that it misinterprets the physical network model when constraining the line flows in the network.
180 Even though the power-flow equations in (12)-(14) are exact when the shunt capacitances are considered as nodal injections, the constraint (16) is imposed on a fictitious current flow across the longitudinal component of the lines, thus *does not* account for the current flow toward the shunt elements. Therefore, the optimum of problem (12)-(18) can be such that the line ampacity constraint is
185 violated.

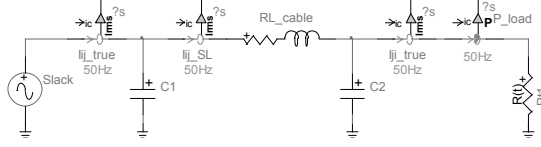


Fig. 1: The test network used for the numerical comparison of the current flows at the sending/receiving end of the lines and the current flow along the longitudinal line impedance.

Table 1: Parameters of the test network in Fig.1

Parameter	Value
Network rated voltage, $V(\text{kV})$	15
Line parameters, $R(\text{Ohms})$, $L(\text{H})$, $C(\text{uF})$	(1,0.003,0.54)

To better clarify why this occurs, we use a single-branch toy network, as shown in Fig. 1. The line parameters, as well as the base values of the system are given in Table 1. A purely resistive load is connected to bus 2 that we vary linearly in the range of $[100 - 10000]\text{Ohms}$ in order to numerically quantify the mismatch between those quantities. We measure the current flows at the two ends of the line, as well as the flow along the longitudinal impedance of the line. Fig. 2 shows the measured quantities as a function of the load. It can be observed that the current flowing across the longitudinal impedance of the line under-estimates the actual current flow in the receiving end of the line.

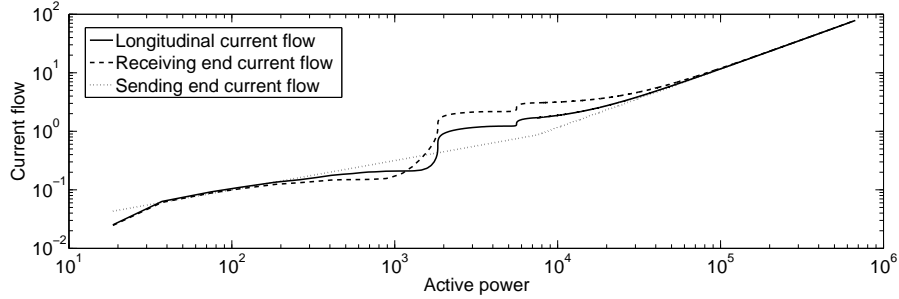


Fig. 2: Current flows at the sending/receiving end of the line and along the longitudinal line impedance (log-log scale).

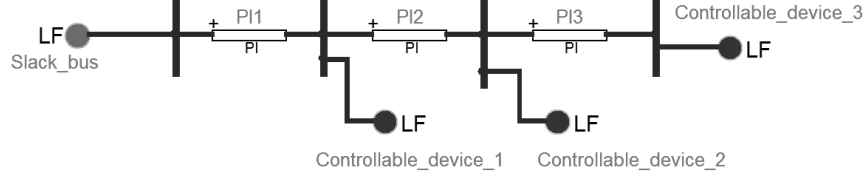


Fig. 3: Network used in the study of the Farivar-Low OPF formulation.

As a consequence, in the Farivar-Low formulation setting the limit on the longitudinal current flow below the line ampacity does not guarantee that the actual line current will respect this limit. In order to illustrate such a scenario, we consider yet another simple test network shown in Fig. 3. All the network lines are built by using the same values of resistance, reactance and capacitance per km, but by assuming different values of their length⁴. We assume a first test case where the controllable device connected to bus 4 is a generator, whereas controllable loads are connected to buses 2 and 3. The network characteristics, the base values, the capability limits of the controllable resources⁵, and the voltage and ampacity bounds are provided in Table 7. We assume that the controllable generation operates at a unity power factor. The problem in (12)-(18) is formulated and solved in Matlab. The objective function accounts for loss minimization, as well as utility maximization of the controllable generation units:

$$\min_{\bar{S}_g, \bar{S}_\ell, |\bar{V}_b|, |\bar{I}_\ell|} - \sum_{g \in \mathcal{G}} \text{Re}(\bar{S}_g) + \sum_{\ell \in \mathcal{L}} \text{Re}(\bar{Y}_\ell) |\bar{I}_\ell|^2 \quad (19)$$

195 In order to investigate the order of magnitude of the violation of the ampacity constraint, we solve the OPF problem for various line lengths and network voltage-rated values. In particular, we assume that the line lengths are uniformly multiplied by a factor in the range $[1.25 - 7.5]$ (while keeping the network voltage rated value to its nominal value) and the network voltage rated value varies in

⁴Typical values of medium-voltage underground cables are considered for the resistance, reactance and shunt capacitances of the lines.

⁵The upper bounds of the active and reactive power of the loads are considered to be infinite, as required in the Farivar-Low formulation.

Table 2: Parameters of the test network in Fig.3 used for the investigation of the line ampacity limit violation

Parameter	Value
Network rated voltage and base power, $V(\text{kV}), S(\text{MVA})$	24.9,5
Line parameters, $R(\text{Ohms/km}), L(\text{mH/km}), C(\text{uF/km})$	(0.193,0.38,0.24)
$[P_{g_{min}}, P_{g_{max}}]$ (MW)	[0, 2]
$P_{c_{min}}$ (MW) (bus2, bus3)	(0.05, 0.06)
$Q_{c_{min}}$ (Mvar) (bus2, bus3)	(0.03, 0.027)
$[V_{min}, V_{max}]$ (p.u)	[0.9, 1.1]
I_{max} (A)	80

the range $[15 - 45]kV$ (while keeping the line lengths to their nominal values). Once the optimal solution is computed in each case, we calculate the actual current flows in the sending/receiving end of the lines and we compute the maximum constraint violation. The results are shown in Fig. 4. As the line length increases, the current flowing toward the shunt capacitors increases, thus neglecting its contribution to the line flow leads to significant violations of the ampacity limit. At 7.5 times the initial line length, the violation reaches a value of 18.4%. The effect of the network voltage-rated value is similar, with a maximum constraint violation of 25% when the voltage value is 45kV.

In addition to the effect of the line lengths and the network voltage-rated value, we study the effect of the network operating point on the ampacity violation. To this end, we consider a second test case where the controllable device connected to bus 4 is a load and generators are connected to buses 2 and 3. The capability limits of the controllable resources are provided in Table 3. For this setting, Fig. 5 shows the solution of the Farivar-Low OPF problem, namely current flows at the receiving/sending end of the network lines, as well as across the longitudinal impedance. We can observe that the maximum violation of the ampacity constraint is in the order of 39.6%.

In order to avoid current flows that exceed the lines' ampacity limits, i.e., in

Table 3: Parameters of the test network in Fig.3 used for the investigation of the network operating point on the line ampacity limit violation

Parameter	Value
$[P_{gmin}, P_{gmax}]$ (MW) (bus 2)	$[0, 0.01]$
$[P_{gmin}, P_{gmax}]$ (MW) (bus 3)	$[0, 0.012]$
(P_{cmin}, Q_{cmin}) (MW, Mvar) (bus 4)	0.3, 0.15

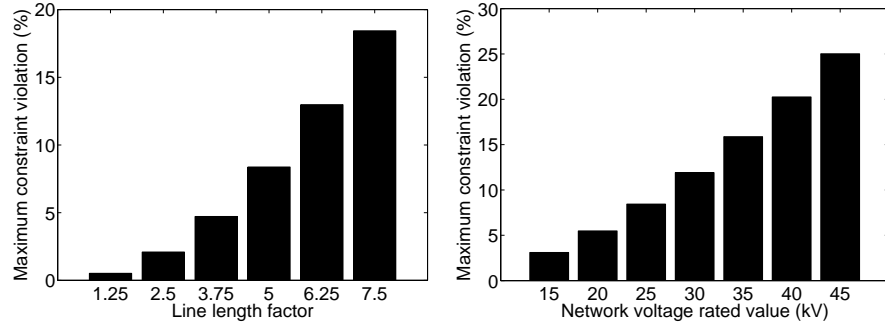


Fig. 4: Maximum ampacity constraint violation as a function of the line lengths and the network voltage rated value.

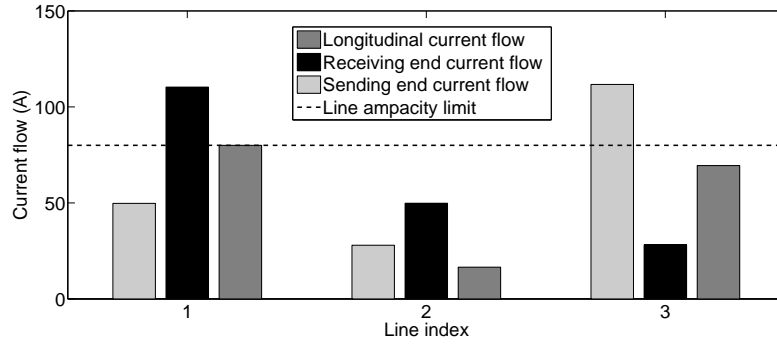


Fig. 5: Farivar-Low OPF solution for the current flows at the sending/receiving end of the network lines and across the longitudinal line impedance under heavy consumption and light generation conditions.

order to use the BFM in an accurate way, the Farivar-Low formulation should
 220 either consider the actual current flows in the receiving/sending ends of the lines
 as optimization variables, or should add the contribution of the current flows
 toward the shunt elements of the lines to the longitudinal current flow in the
 inequality constraint (16). By adopting either of the two approaches, however,
 (12)-(18) can no longer be solved efficiently as proposed in [1, 2]. Therefore, the
 225 generic OPF problem cannot be convexified by using Farivar-Low's approach.

3.3. On the Assumptions Required for the Exactness of the Farivar-Low Relaxation

In addition to the aforementioned fundamental problem, which is related
 to the physical network model, Farivar and Low require specific assumptions
 230 to hold in order to prove the exactness of the proposed relaxations. Several of
 these assumptions are too strong and not realistic.

To begin with, the OPF formulation in [1, 2] assumes controllability of both
 loads and generators in the network buses and, in particular, assumes rectangular
 bounds on the powers of loads/generators. This is quite a strong assumption,
 235 as usually the DNO has very few specific control points available in the network
 with capability curves that are typically more complex and that account, among
 others, for capabilities of power electronics and limitations of machinery. An
 even more serious limitation is that the Farivar-Low model considers no upper
 bounds on the controllable loads in order to prove the exactness of the proposed
 240 relaxation. This implies that in cases where excessive production of the generators
 causes violations of the voltage or line-flows limits, local demand is invoked
 to compensate for the increased generation. In order to illustrate such a setting
 and to show that the result of the OPF problem can result in unrealistic values
 for demand, we consider the same network in Fig. 3 and we assume that there
 245 is high penetration of distributed generation and a low demand. The values
 of loads and generation, as well as the corresponding limits are shown in Table 4.
 Solving the optimization problem and considering infinite upper bounds
 on the demand results in load values that are significantly increased, compared

Table 4: Parameters of the test network in Fig.3 used for the investigation of the unboundedness of the consumption

Parameter	Value
$[P_{gmin}, P_{gmax}]$ (MW)	$[0, 1.2]$
(P_{cmin}, Q_{cmin}) (MW,Mvar) (buses 2,3)	$(0.0125, 0.0026)$

to the minimum values shown in Table 4. The resulting optimal power points
250 are shown in Fig. 6. We show in black the initial values for active and reactive
power of loads and generation (corresponding to the values of Table 4), and in
gray the results of the OPF solution (when not accounting for upper bounds
on loads). It is worth observing that the optimal active power consumption of
bus 3 is increased 23.6 times and the reactive power consumption at buses 2
255 and 3 is increased 85.3 and 92 times, respectively. In a realistic setting, even
if part of the demand in the network is controllable, the amount of available
demand-response is limited and such an increase in the consumption is most
likely not possible. Therefore, in such a case, the congestion and voltage prob-
lems should be solved by properly controlling the generator within its capability
260 limits. In addition to this, typically, the active and reactive power consumption
should be linked via the corresponding power factor. We observe, however, that
the OPF solution in this scenario results in very large values for the reactive
power consumption and, in particular, the power factor of Bus 2 is 0.03 after
the OPF solution, whereas initially its value is 0.98. In an attempt to relax this
265 assumption, Farivar and Low claim that the infinite upper bound on the loads,
when not applicable, can be replaced by equivalent conditions [42]. However,
not only are these conditions unrealistic, they are also not applicable in our
context as they require no upper bound on the voltage magnitudes. This is in
contradiction with the actual problem we target, i.e., voltage rise due to high
270 penetration of renewable energy resources.

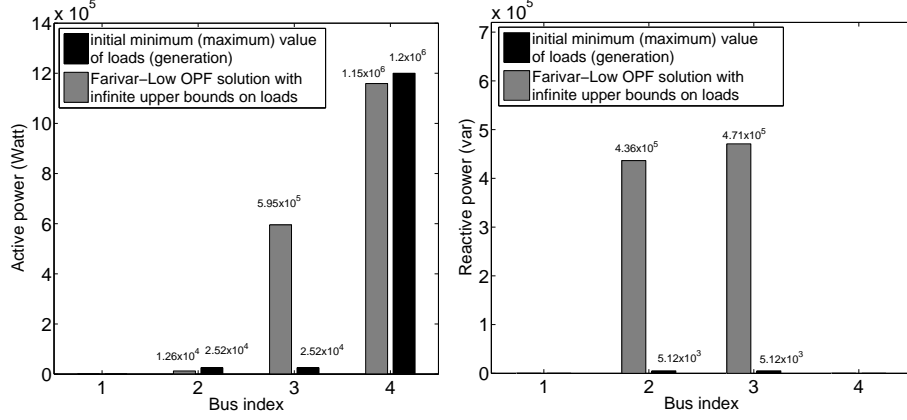


Fig. 6: Optimal solution of the Farivar-Low OPF formulation for the active and reactive power set-points when upper bounds on loads are infinite.

3.4. On the Extension of the SOCP Relaxation to Networks with Lines Modeled as π -equivalents

In this paragraph, we discuss two different approaches that can be used to extend the initial formulation in (12)-(18) in order to account for the shunt elements of the lines. We show through concrete examples that extending the Farivar-Low approach to a system model that is correctly represented cannot guarantee the exactness of the SOCP relaxation and, thus, the retrieval of a feasible OPF solution.

A straightforward way to account for the line ampacity constraints in (16) is to re-write a new set of line constraints for the case of π -model lines while keeping the same branch flow variables. In this case, the line constraints are reformulated as follows:

$$|\bar{I}_\ell|^2 + |\bar{Y}_{\ell_0^+}|^2 |\bar{V}_{\beta(\ell^+)}|^2 + 2\text{Real}(\bar{Y}_{\ell_0^+} \bar{S}_\ell) \leq I_{\ell_{max}}^2, \forall \ell \in \mathcal{L} \quad (20)$$

$$|\bar{I}_\ell|^2 + |\bar{Y}_{\ell_0^-}|^2 |\bar{V}_{\beta(\ell^-)}|^2 + 2\text{Real}(\bar{Y}_{\ell_0^-} (\bar{Y}_\ell^{-1} |\bar{I}_\ell|^2 - \bar{S}_\ell)) \leq I_{\ell_{max}}^2, \forall \ell \in \mathcal{L} \quad (21)$$

It is worth noting that these new constraints, that account also for the line flows towards the shunt elements, are convex and can be added to Farivar and

Table 5: Parameters of the test network in Fig.3

Parameter	Value
Network rated voltage and base power, $V(\text{kV}), S(\text{MVA})$	24.9,5
Line parameters, $R(\text{Ohms/km}), L(\text{mH/km}), C(\text{uF/km})$	(0.193,0.38,0.24)
$P_{g_{max}}$ (bus2, bus3)(MW)	(1, 1.2)
$P_{c_{min}}$ (MW) (bus4)	0.1
$Q_{c_{min}}$ (Mvar) (bus4)	0.05
$[V_{min}, V_{max}]$ (p.u)	[0.9, 1.1]
I_{max} (A)	80

285 Lows' OPF formulation. However, this doesn't mean that the optimal solution of the relaxed SOCP problem is guaranteed to be a physically feasible one, in other words, the theorem in [1] does not hold here.

To support this claim, let us consider the following simple example. We use once again the same simple test network shown in Fig. 3. We assume a test case
 290 where the controllable device connected to bus 4 is a load, whereas controllable generators are connected to buses 2 and 3. The network characteristics, the base values, the capability limits of the controllable resources, and the voltage and ampacity bounds are provided in Table 5. We assume that the controllable generators operate at a unity power factor. Note that the upper bounds for the
 295 loads are considered infinite as required in the original formulation of Farivar and Low.

We solve the problem in Matlab and the resulting values for the SOCP inequalities for each network line are shown in Table. 6. In this case, after the solution of the OPF problem not all the inequalities in (13) are satisfied
 300 with equality, namely the SOCP relaxation is inexact, therefore, the obtained solution has no physical meaning and a physically feasible solution cannot be recovered.

A second way to extend the approach in [1] to networks with lines represented as π -equivalents is to reconstruct the BFM in order to include the shunt elements

Table 6: SOCP inequalities in (13)

Line	Value
1 – 2	$1.7E - 16$
2 – 3	-0.0461
3 – 4	$1.3E - 16$

of the lines. To this end, we consider an undirected graph $G = (\mathcal{N}, \mathcal{E})$. \mathcal{N} and \mathcal{E} represent the set of nodes and lines respectively. The shunt elements of a line ℓ are denoted by $\bar{Y}_{\ell_0^+}$ and $\bar{Y}_{\ell_0^-}$. Note that for passive, reciprocal, two-port circuit equivalents, these two elements must be identical. The OPF problem in (12)-(18) is reformulated as:

$$\min_{\substack{\bar{S}_g, \bar{S}_c, S_{\ell^+}, |\bar{I}_{\ell^+}|^2, |\bar{V}_{\beta(\ell^+)}|^2, \\ S_{\ell^-}, |\bar{I}_{\ell^-}|^2, |\bar{V}_{\beta(\ell^-)}|^2}} C_g(\bar{S}_g) + \sum_{c \in \mathcal{C}} C_c(\bar{S}_c) \quad (22)$$

$$\text{subject to: } \sum_{g \in b} \bar{S}_g - \sum_{c \in b} \bar{S}_c - \sum_{\beta(\ell^+)=b} \bar{S}_{\ell^+} - \sum_{\beta(\ell^-)=b} \bar{S}_{\ell^-} = 0, \forall b \in \mathcal{B} \quad (23)$$

$$|S_{\ell^+}|^2 - |\bar{V}_{\beta(\ell^+)}|^2 |\bar{I}_{\ell^+}|^2 \leq 0, \quad |S_{\ell^-}|^2 - |\bar{V}_{\beta(\ell^-)}|^2 |\bar{I}_{\ell^-}|^2 \leq 0, \quad \forall \ell \in \mathcal{L} \quad (24)$$

$$|\alpha_{\ell^+}|^2 |\bar{V}_{\beta(\ell^+)}|^2 - |\bar{V}_{\beta(\ell^-)}|^2 = 2\text{Re}(\alpha_{\ell^+} \underline{Y}_{\ell}^{-1} S_{\ell^+}) - |\bar{Y}_{\ell}^{-1}| |\bar{I}_{\ell^+}|^2, \quad \forall \ell \in \mathcal{L} \quad (25)$$

$$|\alpha_{\ell^-}|^2 |\bar{V}_{\beta(\ell^-)}|^2 - |\bar{V}_{\beta(\ell^+)}|^2 = 2\text{Re}(\alpha_{\ell^-} \underline{Y}_{\ell}^{-1} S_{\ell^-}) - |\bar{Y}_{\ell}^{-1}| |\bar{I}_{\ell^-}|^2, \quad \forall \ell \in \mathcal{L} \quad (26)$$

$$\text{where } \alpha_{\ell^+} := 1 + \bar{Y}_{\ell}^{-1} \bar{Y}_{\ell_0^+}, \alpha_{\ell^-} := 1 + \bar{Y}_{\ell}^{-1} \bar{Y}_{\ell_0^-}.$$

At this point it is important to note that, in order to recover a solution
 305 of the original ACOPF problem, we need to recover the line angle from the
 solution of the above problem in a way similar to [1]. In the original paper
 of Farivar and Low, it is shown that for radial distribution networks the angle
 relaxation step is always exact. On the contrary, in the formulation above, both
 angles $\beta_{\ell^+} = \angle(\alpha_{\ell^+} |\bar{V}_{\beta(\ell^+)}|^2 - \underline{Y}_{\ell}^{-1} \bar{S}_{\ell^+})$ and $\beta_{\ell^-} = \angle(\alpha_{\ell^-} |\bar{V}_{\beta(\ell^-)}|^2 - \underline{Y}_{\ell}^{-1} \bar{S}_{\ell^-})$
 310 are defined. In order for a solution to be physically meaningful, namely the
 angle relaxation step to be exact, these line angles should satisfy $\beta_{\ell^+} + \beta_{\ell^-} = 0$.
 However, there is no guarantee that this will occur in the obtained solution. In
 fact, as we show in the example that follows the angle relaxation is not exact
 when using this formulation even in the case of radial networks.

Table 7: Parameters of the test network in Fig.3

Parameter	Value
Network rated voltage and base power, $V(\text{kV}), S(\text{MVA})$	24.9,5
Line parameters, $R(\text{Ohms/km}), L(\text{mH/km}), C(\text{uF/km})$	(0.193,0.38,0.24)
$[P_{gmin}, P_{gmax}]$ (MW)	[0, 2]
P_{cmin} (MW) (bus2, bus3)	(0.05, 0.06)
Q_{cmin} (Mvar) (bus2, bus3)	(0.03, 0.027)
$[V_{min}, V_{max}]$ (p.u)	[0.9, 1.1]
I_{max} (A)	80

315 To support the above claim, we consider the same simple test network shown in Fig. 3. For the sake of simplicity, we assume a test case where the controllable device connected to bus 4 is a generator, whereas controllable loads are connected to buses 2 and 3. The network characteristics, the base values, the capability limits of the controllable resources, and the voltage and ampacity
320 bounds are provided in Table 7. We assume that the controllable generation operates at a unity power factor. Note that the upper bounds for the loads are considered infinite as in the original paper of Farivar and Low.

The objective function has two terms, namely loss minimization and utility maximization of the controllable generation unit:

$$\min_{\substack{\bar{S}_g, \bar{S}_c, \bar{S}_{\ell+}, |\bar{I}_{\ell+}|^2, |\bar{V}_{\ell+}|^2, \\ \bar{S}_{\ell-}, |\bar{I}_{\ell-}|^2, |\bar{V}_{\ell-}|^2}} \sum_{\ell \in \mathcal{L}} \text{real}(\bar{Y}_{\ell}^{-1})(|\bar{I}_{\ell+}|^2 + |\bar{V}_{\ell+}|^2 \bar{Y}_{\ell_0^+}^2 - \text{imag}(\bar{S}_{\ell+})) + \quad (27)$$

$$\text{real}(\bar{Y}_{\ell}^{-1})(|\bar{I}_{\ell-}|^2 + |\bar{V}_{\ell-}|^2 \bar{Y}_{\ell_0^-}^2 - \text{imag}(\bar{S}_{\ell-})) - \sum_{g \in \mathcal{G}} \text{real}(\bar{S}_g) \quad (28)$$

It is worth mentioning that in view of the new formulation, the current used
325 for the real losses computation is no longer represented by the variable $|\bar{I}_{\ell}|^2$, but needs to be computed as the difference between the current flowing from one end of the line to the other and the current flowing towards the shunt elements. This has two implications. First, the current across the series admittance can

be computed twice using $|\bar{I}_{\ell+}|^2$ or $|\bar{I}_{\ell-}|^2$. Neglecting one of the two currents in
 330 the objective function results in a non-exact SOCP relaxation. Second, computing
 the longitudinal component of the current results in the objective function
 not being independent of the power flow variables, which is one of the assumptions
 used in the original paper of Farivar and Low to prove exactness of their
 proposed relaxation.

335 In this case, after the solution of the OPF problem the inequalities in (24)
 are satisfied with equality, namely the SOCP relaxation is exact. The values for
 the two inequalities for each network line are shown in Fig. 7. For the same test
 case, we obtain the line angles $\beta_{\ell+}$ and $\beta_{\ell-}$. The results are shown in Fig. 8. One
 can clearly observe that the obtained line angles do not satisfy $\beta_{\ell+} + \beta_{\ell-} = 0$
 340 and, therefore, the obtained solution has, again, no physical meaning.

The aforementioned examples indicate that the proposed Farivar-Low relaxation
 cannot be trivially extended to lines represented as π -model equivalents
 even with convex constraints applied to the line exact π -model. Overall, the fun-
 345 damental problems with the Farivar-Low approach, as well as with the several
 additional assumptions, prohibit its application to the generic OPF problem.
 As a consequence, there is a need to design algorithms that target the original

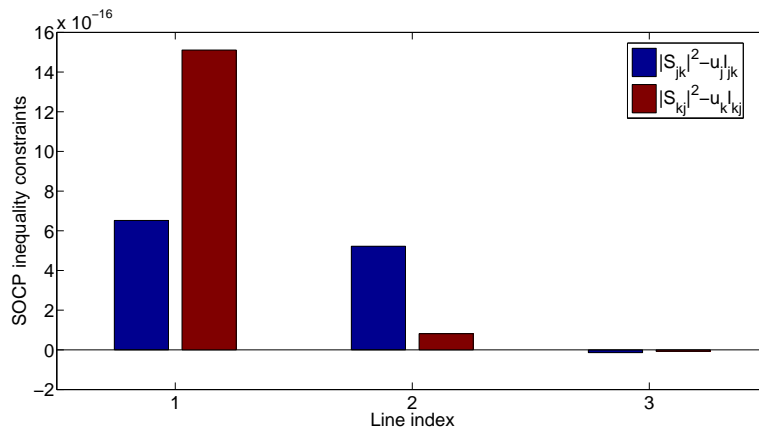


Fig. 7: The relaxed inequalities values for the problem (22)-(26).

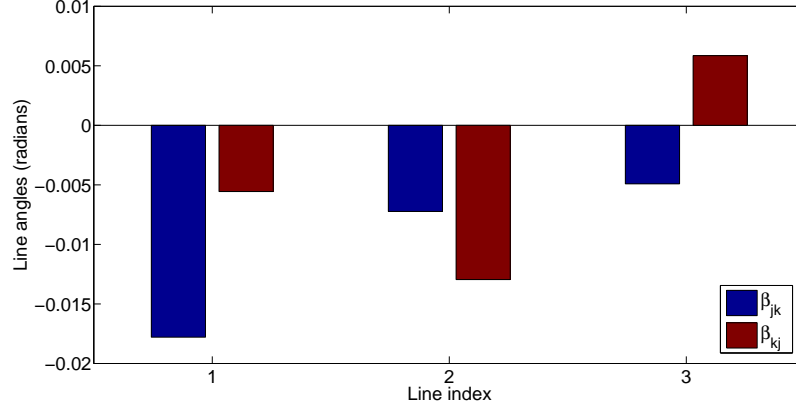


Fig. 8: The line angles obtained after the OPF solution of problem (22)-(26).

non-approximated OPF problem that remains inherently non-convex. Recent trends are in favor of using ADMM for the solution of the OPF problem. Even though ADMM requires the underlying problem to be convex in order to guarantee convergence, it has been applied also to the case of non-convex AC OPF problems with promising convergence performance (e.g., [21, 24]). In what follows we first present the ADMM solution of the problem in (1)-(9) and then we highlight specific scenarios for which ADMM fails to converge when applied to the non-approximated OPF problem.

4. On the Application of ADMM for the Solution of the OPF Problem

4.1. ADMM-based Solution of the OPF Problem

The ADMM-based solution of the OPF problem requires that the control variables are split into two separate groups and that the objective function is separable across this splitting [45]. To this end, we introduce additional slack variables, \bar{z} , for the devices' and loads' power injections and for the line power flows and we reformulate the OPF problem as follows⁶:

⁶In what follows we assume that demand is non-controllable. Also, as in [20] the constraints (3),(9) are considered internal constraints of the lines and devices respectively and

$$\min_{\substack{\bar{S}_g, \bar{z}_g, \bar{S}_c, \bar{z}_c, \bar{S}_{\ell^+}, \bar{z}_{\ell^+}, \bar{S}_{\ell^-}, \\ \bar{z}_{\ell^-}, \bar{E}_{\ell^+}, \bar{E}_{\ell^-}, \bar{I}_{\ell^+}, \bar{I}_{\ell^-}, \bar{V}_b}} - \sum_g U_g(\text{Re}(\bar{S}_g)) + \sum_b J_V(|\bar{V}_b|) + \quad (29)$$

$$\sum_{\ell} J_I(|\bar{I}_{\ell}^+|, |\bar{I}_{\ell}^-|) + \sum_b \phi\left(\sum_{g \in b} \bar{z}_g - \sum_{c \in b} \bar{z}_c + \sum_{\beta(\ell^+)=b} \bar{z}_{\ell^+} + \sum_{\beta(\ell^-)=b} \bar{z}_{\ell^-}\right)$$

subject to: $\bar{S}_g = \bar{z}_g, \forall g \in \mathcal{G}$, and $\bar{S}_c = \bar{z}_c, \forall c \in \mathcal{C}$ (30)

$$\bar{S}_{\ell^+} = \bar{z}_{\ell^+}, \quad \text{and} \quad \bar{S}_{\ell^-} = \bar{z}_{\ell^-}, \quad \forall \ell \in \mathcal{L} \quad (31)$$

$$\bar{E}_{\ell^+} = \bar{V}_{\beta(\ell^+)}, \quad \text{and} \quad \bar{E}_{\ell^-} = \bar{V}_{\beta(\ell^-)}, \quad \forall \ell \in \mathcal{L} \quad (32)$$

where ϕ is the characteristic function of the set $\{\bar{x} \in \mathbb{C} : \bar{x} = 0\}$, J_V is a penalty function with value 0 if $V_{\min} \leq |\bar{V}_b| \leq V_{\max}$ and ∞ otherwise and J_I is a penalty function with value 0 if $\max(|\bar{I}_{\ell}^+|, |\bar{I}_{\ell}^-|) \leq I_{\ell_{\max}}$ and ∞ otherwise. 365

The augmented Lagrangian for this problem is as follows:

$$\begin{aligned} L_{\omega}(\bar{S}_g, \bar{S}_c, \bar{S}_{\ell^+}, \bar{S}_{\ell^-}, \bar{E}_{\ell^+}, \bar{E}_{\ell^-}, \bar{I}_{\ell^+}, \bar{I}_{\ell^-}, \bar{z}_g, \bar{z}_c, \bar{z}_{\ell^+}, \bar{z}_{\ell^-}, \bar{V}_b, \bar{\mu}, \bar{\nu}, \bar{\lambda}) \\ = - \sum_g U_g(\text{Re}(\bar{S}_g)) + \sum_b J_V(|\bar{V}_b|) + \sum_{\ell} J_I(|\bar{I}_{\ell}^+|, |\bar{I}_{\ell}^-|) \\ + \sum_b \phi\left(\sum_{g \in b} \bar{z}_g - \sum_{c \in b} \bar{z}_c + \sum_{\beta(\ell^+)=b} \bar{z}_{\ell^+} + \sum_{\beta(\ell^-)=b} \bar{z}_{\ell^-}\right) \\ + \frac{\omega}{2} \left\{ \sum_{\ell} |\bar{E}_{\ell^+} - \bar{V}_{\beta(\ell^+)} + \bar{\mu}_{\ell}|^2 + \sum_{\ell} |\bar{E}_{\ell^-} - \bar{V}_{\beta(\ell^-)} + \bar{\nu}_{\ell}|^2 \right. \\ + \sum_g |\bar{S}_g - \bar{z}_g + \bar{\lambda}_g|^2 + \sum_c |\bar{S}_c - \bar{z}_c + \bar{\lambda}_c|^2 \\ \left. + \sum_{\ell} |\bar{S}_{\ell^+} - \bar{z}_{\ell^+} + \bar{\lambda}_{\ell^+}|^2 + \sum_{\ell} |\bar{S}_{\ell^-} - \bar{z}_{\ell^-} + \bar{\lambda}_{\ell^-}|^2 \right\} \quad (33) \end{aligned}$$

where $\bar{\mu}, \bar{\nu}, \bar{\lambda}$ are the lagrange multipliers associated with the equality constraints (30)-(32).

The ADMM algorithm at the k -th iteration consists of the following steps:

1. First, all the devices, loads and lines update in parallel the primary variables, and their internal variables, i.e., $(\bar{S}_g, \bar{S}_c, \bar{S}_{\ell^+}, \bar{S}_{\ell^-}, \bar{E}_{\ell^+}, \bar{E}_{\ell^-}, \bar{I}_{\ell^+}, \bar{I}_{\ell^-})$

$\bar{I}_{\ell}^+, \bar{I}_{\ell}^-$ are internal variables of the lines.

with the secondary variables, and the dual variables fixed ⁷:

For each network line ℓ :

$$\begin{aligned}
& (\bar{S}_{\ell+}^{k+1}, \bar{S}_{\ell-}^{k+1}, \bar{E}_{\ell+}^{k+1}, \bar{E}_{\ell-}^{k+1}, \bar{I}_{\ell+}^{k+1}, \bar{I}_{\ell-}^{k+1}) = \\
& \underset{\bar{S}_{\ell+}, \bar{S}_{\ell-}, \bar{E}_{\ell+}, \bar{E}_{\ell-}, \bar{I}_{\ell+}, \bar{I}_{\ell-}}{\operatorname{argmin}} J_I(|\bar{I}_{\ell+}^+|, |\bar{I}_{\ell-}^-|) + \\
& \frac{\omega}{2} (|\bar{E}_{\ell+} - \bar{V}_{\beta(\ell+)}^k + \bar{\mu}_{\ell}^k|^2 + |\bar{E}_{\ell-} - \bar{V}_{\beta(\ell-)}^k + \bar{\nu}_{\ell}^k|^2 \\
& + |\bar{S}_{\ell+} - \bar{z}_{\ell+}^k + \bar{\lambda}_{\ell+}^k|^2 + |\bar{S}_{\ell-} - \bar{z}_{\ell-}^k + \bar{\lambda}_{\ell-}^k|^2)
\end{aligned} \tag{34}$$

$$\text{subject to: } \bar{S}_{\ell+} = \bar{E}_{\ell+} \bar{I}_{\ell+} \quad \text{and} \quad \bar{S}_{\ell-} = \bar{E}_{\ell-} \bar{I}_{\ell-} \tag{35}$$

$$\bar{I}_{\ell+} = \bar{Y}_{\ell}(\bar{E}_{\ell+} - \bar{E}_{\ell-}) + \bar{Y}_{\ell_0^+} \bar{E}_{\ell+} \tag{36}$$

$$\bar{I}_{\ell-} = \bar{Y}_{\ell}(\bar{E}_{\ell-} - \bar{E}_{\ell+}) + \bar{Y}_{\ell_0^-} \bar{E}_{\ell-} \tag{37}$$

For each device g : (38)

$$\bar{S}_g^{k+1} = \underset{\bar{S}_g}{\operatorname{argmin}} -U_g(\operatorname{Re}(\bar{S}_g)) + \frac{\omega}{2} (|\bar{S}_g - \bar{z}_g^k + \bar{\lambda}_g^k|^2)$$

subject to: $\bar{S}_g \in \mathcal{H}_g$

$$\text{For each load } c: \bar{S}_c^{k+1} = \bar{S}_c \tag{39}$$

2. Then, by using the updated primary variables, the secondary variables are updated, i.e., (\bar{z}, \bar{V}_b) , on a bus level. We denote by \bar{z}_b the vector of complex powers of all the devices, loads and lines that are connected to bus b , i.e., $\bar{z}_b \triangleq (\bar{z}_{g:g \in b}, \bar{z}_{c:c \in b}, \bar{z}_{\ell+: \beta(\ell+)=b}, \bar{z}_{\ell-: \beta(\ell-)=b})$:

$$\begin{aligned}
\bar{z}_b^{k+1} = & \underset{\bar{z}_b}{\operatorname{argmin}} (\phi(\sum_{g \in b} \bar{z}_g - \sum_{c \in b} \bar{z}_c + \sum_{\beta(\ell+)=b} \bar{z}_{\ell+} + \sum_{\beta(\ell-)=b} \bar{z}_{\ell-})) \\
& + \frac{\omega}{2} \{ \sum_{g \in b} |\bar{S}_g^{k+1} - \bar{z}_g + \bar{\lambda}_g^k|^2 + \sum_{c \in b} |\bar{S}_c^{k+1} - \bar{z}_c + \bar{\lambda}_c^k|^2 \\
& + \sum_{\beta(\ell+)=b} |\bar{S}_{\ell+}^{k+1} - \bar{z}_{\ell+} + \bar{\lambda}_{\ell+}^k|^2 + \sum_{\beta(\ell-)=b} |\bar{S}_{\ell-}^{k+1} - \bar{z}_{\ell-} + \bar{\lambda}_{\ell-}^k|^2 \}
\end{aligned} \tag{40}$$

⁷Note that demand is not controllable, hence the loads do not require the solution of an optimization problem to update their power consumption.

$$\begin{aligned} \bar{V}_b^{k+1} = \underset{\bar{V}_b}{\operatorname{argmin}} & (J(\bar{V}_b) + \frac{\omega}{2} \{ \sum_{\beta(\ell^+)=b} |\bar{E}_{\ell^+}^{k+1} - \bar{V}_b + \bar{\mu}_\ell^k|^2 \\ & + \sum_{\beta(\ell^-)=b} |\bar{E}_{\ell^-}^{k+1} - \bar{V}_b + \bar{\nu}_\ell^k|^2 \}) \end{aligned} \quad (41)$$

3. Finally, dual variables, i.e., $\bar{\mu}, \bar{\nu}, \bar{\lambda}$ are updated:

$$\bar{\mu}_\ell^{k+1} = \bar{\mu}_\ell^k + (\bar{E}_{\ell^+}^{k+1} - \bar{V}_{\beta(\ell^+)}) \quad (42)$$

$$\bar{\nu}_\ell^{k+1} = \bar{\nu}_\ell^k + (\bar{E}_{\ell^-}^{k+1} - \bar{V}_{\beta(\ell^-)}) \quad (43)$$

$$\bar{\lambda}_g^{k+1} = \bar{\lambda}_g^k + (\bar{S}_g^{k+1} - \bar{z}_g^{k+1}) \quad (44)$$

$$\bar{\lambda}_c^{k+1} = \bar{\lambda}_c^k + (\bar{S}_c^{k+1} - \bar{z}_c^{k+1}) \quad (45)$$

$$\bar{\lambda}_{\ell^+}^{k+1} = \bar{\lambda}_{\ell^+}^k + (\bar{S}_{\ell^+}^{k+1} - \bar{z}_{\ell^+}^{k+1}) \quad (46)$$

$$\bar{\lambda}_{\ell^-}^{k+1} = \bar{\lambda}_{\ell^-}^k + (\bar{S}_{\ell^-}^{k+1} - \bar{z}_{\ell^-}^{k+1}) \quad (47)$$

The stopping criterion for this algorithm is that the primal and dual residuals (defined as in [45]) are less than a small predefined tolerance or that a maximum number of iterations has been reached.

In what follows, we show specific scenarios where the ADMM algorithm fails to converge to a solution.

4.2. Investigation of the Convergence of the ADMM-based Solution of the OPF Problem

We consider the same network in Fig. 3. Each network bus, apart from the slack bus, has a load and a generator connected to it. The demand in the network is assumed to be non-controllable, whereas the generators are assumed to be distributed solar panels with typical PV-type capability constraints. For this scenario, the capability limits and the values of loads and generation are given in Table 8. In addition to the loads and generation, we consider that a shunt capacitor is connected to bus 2. In order to model this shunt capacitor, we consider that it is part of the first network line. In particular, we consider that the shunt capacitance on the sending end of the π -model of the line connecting buses 1 and 2 is modified accordingly to account for the shunt capacitor.

We implement and solve the ADMM algorithm in Matlab for two different cases that correspond to two different values of the size of the shunt capacitor (see Table 8). In Case I, even though the OPF problem solved is the non-approximated non-convex one, ADMM converges, within the predefined tolerance, in 411 iterations. The left figure in Fig. 9 shows the objective function value as a function of the number of iterations of ADMM. The left figure in Fig. 10 shows the convergence of the buses' voltage magnitudes and Fig. 11 shows how the primal and dual residuals evolve with the iterations. On the contrary, in Case II, ADMM fails to converge to a solution and reaches the maximum number of iterations. This is shown in Fig. 9 (right), 10 (right) and 12 where the objective function, as well as the residuals and bus voltages are plotted for the last five hundred iterations until the maximum number of iterations is reached; we can observe that they exhibit oscillations.

In what follows we analyze why the ADMM algorithm converges in Case I but fails in Case II. To begin with, the first network line has the peculiarity that the voltage at its receiving end $\bar{E}_{\ell+}$ (i.e., the slack bus voltage) is fixed.⁸ As a consequence, the first equality constraint in (35) becomes linear in the real

Table 8: Parameters of the test network in Fig.3 used for the ADMM-based solution of the OPF problem

Parameter	Value
Generators' power, $ \bar{S}_{i_{gmax}} , i = 2, 3, 4$ (MVA)	0.40, 0.39, 0.46
Generators' power factor, $\cos\phi_{i_g}, i = 2, 3, 4$	0.9
Loads' active power, $P_{i_c}, i = 2, 3, 4$ (MW)	2.76, 2.16, 2.46
Loads' reactive power, $Q_{i_c}, i = 2, 3, 4$ (MW)	1.38, 1.08, 1.23
Shunt capacitor (bus 2), case I and II (uF)	(239, 859)
Penalty term gain, ω	1
Tolerance and maximum number of iterations	$10^{-4}, 10^4$

⁸This holds for all the lines that are connected to the slack bus.

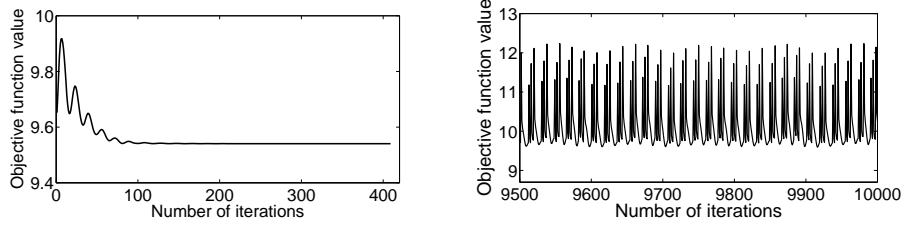


Fig. 9: Objective function value for case I and II (last 500 iterations).

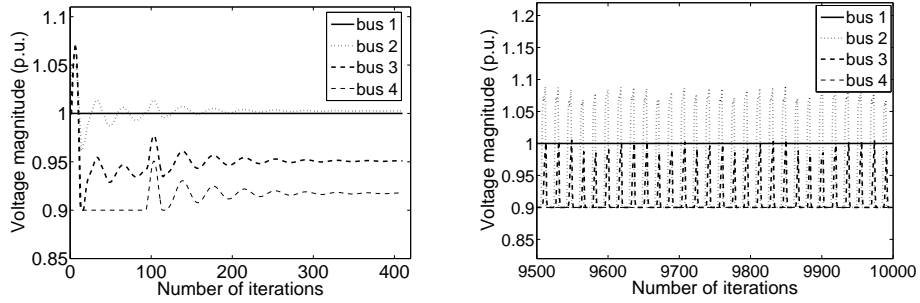


Fig. 10: Voltage magnitude evolution for cases I and II (last 500 iterations).

and imaginary part of the voltage $\bar{E}_{\ell-}$, whereas the second equality constraint in (35) becomes quadratic on the real and imaginary part of the voltage $\bar{E}_{\ell-}$. In fact, the coefficients of the quadratic terms in the latter constraint are $Re(\bar{Y}_{\ell})$ and $-Im(\bar{Y}_{\ell}) - Im(\bar{Y}_{\ell_0-})$ for the real and imaginary parts, respectively. Due to the physics of the network, $Re(\bar{Y}_{\ell})$ and $Im(\bar{Y}_{\ell_0-})$ are positive for a network line and $Im(\bar{Y}_{\ell})$ is negative. Furthermore, typically, the longitudinal reactance

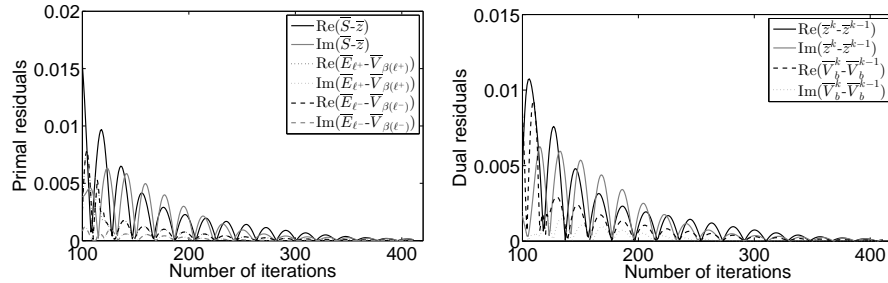


Fig. 11: Norm of the primal/dual residuals for case I (last 311 iterations).

$Im(\bar{Y}_\ell)$ is much larger than the shunt capacitance $Im(\bar{Y}_{\ell_0^-})$ of a network line.
 Therefore, typically the coefficients of both quadratic terms are positive, and
 the line problem in (34) is convex for the lines that are connected to the slack
 bus. This is the case for the Case I. However, in Case II the size of the shunt
 capacitor, connected to bus 2, is such that $Im(\bar{Y}_{\ell_0^-}) > -Im(\bar{Y}_\ell)$, thus the co-
 efficient of the aforementioned quadratic term in (35) is no longer positive and
 the corresponding line problem becomes non-convex.

Apart from the aforementioned case of the shunt capacitor, the ADMM al-
 gorithm also fails to converge to a solution when on-load tap changers (OLTCs)
 are included in the OPF formulation.⁹ In fact, the effect of the OLTCs is simi-
 lar to that of the shunt capacitors, in the sense that the line problem in (34)
 becomes once again non-convex for those lines that are connected to regulating
 transformers. To better understand why this occurs, let us consider a trans-
 former with OLTC capabilities between buses 1 and 2 in the network and let
 us denote the ideal transformer admittance by Y_t and the OLTC ratio by α .
 Then based on the OLTC model in [46], the longitudinal admittance of the first
 network line equals αY_t and the shunt elements of the receiving and sending
 ends of the same line are $\alpha(\alpha - 1)Y_t$ and $(1 - \alpha)Y_t$ respectively. Hence, there is
 an additional control variable, namely the ratio α , that appears in the equality
 constraints (35) of the first network line problem, and both these constraints

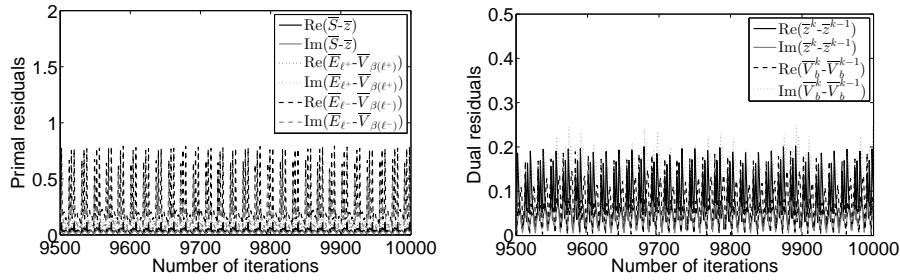


Fig. 12: Norm of the primal/dual residuals for case II (last 500 iterations).

⁹For the sake of brevity we do not include the simulation results for this specific scenario.

become quadratic in \bar{E}_{ℓ^-} and α and non-convex.

430 In this first part of the paper we have focused on investigating the limits
of the branch flow convexification proposed by Farivar-Low in [1, 2] and of the
ADMM-based solution of the OPF problem. In particular, we have discussed
the misinterpretation of the physical model in the Farivar-Low formulation of
the OPF problem and the unrealistic assumptions therein. Finally, we have
435 provided the ADMM-based decomposition of the OPF problem and we have
shown, through specific examples, cases for which the ADMM-based solution of
the non-relaxed OPF problem fails to converge.

References

- [1] M. Farivar, S. H. Low, Branch flow model: Relaxations and convexification
440 - part I, IEEE Trans. on Power Systems 28 (3) (2013) 2554–2564.
- [2] M. Farivar, S. Low, Branch flow model: Relaxations and convexification
- part II, IEEE Trans. on Power Systems 28 (3) (2013) 2565–2572. doi:
10.1109/TPWRS.2013.2255318.
- [3] J. Carpentier, Contribution to the economic dispatch problem, Bulletin de
445 la Société Française des Electriciens 3 (8) (1962) 431–447.
- [4] D. Sun, B. Ashley, B. Brewer, A. Hughes, W. F. Tinney, Optimal power
flow by newton approach, IEEE Trans. on Power Apparatus and Systems
PAS-103 (10) (1984) 2864–2880. doi:10.1109/TPAS.1984.318284.
- [5] D. Gayme, U. Topcu, Optimal power flow with large-scale storage inte-
450 gration, IEEE Trans. on Power Systems 28 (2) (2013) 709–717. doi:
10.1109/TPWRS.2012.2212286.
- [6] M. Adibi, R. Polyak, I. Griva, L. Mili, S. Ammari, Optimal transformer
tap selection using modified barrier-augmented lagrangian method, IEEE
Trans. on Power Systems 18 (1) (2003) 251–257. doi:10.1109/TPWRS.
455 2002.807093.

- [7] C. Lehmkoetter, Security constrained optimal power flow for an economical operation of FACTS-devices in liberalized energy markets, *IEEE Trans. on Power Delivery* 17 (2) (2002) 603–608. doi:10.1109/61.997946.
- [8] B. Hayes, I. Hernando-Gil, A. Collin, G. Harrison, S. Djokić, Optimal power
460 flow for maximizing network benefits from demand-side management, *IEEE Trans. on Power Systems* 29 (4) (2014) 1739–1747. doi:10.1109/TPWRS.2014.2298894.
- [9] R. Jabr, Optimal power flow using an extended conic quadratic formulation, *IEEE Trans. on Power Systems* 23 (3) (2008) 1000–1008. doi:10.1109/
465 TPWRS.2008.926439.
- [10] B. C. Lesieutre, I. Hiskens, et al., Convexity of the set of feasible injections and revenue adequacy in FTR markets, *IEEE Trans. on Power Systems* 20 (4) 1790–1798.
- [11] I. A. Hiskens, R. J. Davy, Exploring the power flow solution space boundary,
470 *IEEE Trans. on Power Systems* 16 (3) (2001) 389–395.
- [12] Y. Makarov, Z.-Y. Dong, D. Hill, On convexity of power flow feasibility boundary, *IEEE Trans. on Power Systems* 23 (2) (2008) 811–813. doi:10.1109/TPWRS.2008.919307.
- [13] J. A. Momoh, M. El-Hawary, R. Adapa, A review of selected optimal power
475 flow literature to 1993. part I: Nonlinear and quadratic programming approaches, *IEEE Trans. on Power Systems* 14 (1) (1999) 96–104.
- [14] J. A. Momoh, M. El-Hawary, R. Adapa, A review of selected optimal power flow literature to 1993. part II: Newton, linear programming and interior point methods, *IEEE Trans. on Power Systems* 14 (1) (1999) 105–111.
- [15] Z. Qiu, G. Deconinck, R. Belmans, A literature survey of optimal power flow
480 problems in the electricity market context, in: *Power Systems Conference and Exposition, PSCE. IEEE/PES, IEEE, 2009*, pp. 1–6.

- [16] S. Bolognani, R. Carli, G. Cavraro, S. Zampieri, A distributed control strategy for optimal reactive power flow with power constraints, in: 52nd Annual Conference on Decision and Control (CDC), IEEE, 2013, pp. 4644–4649.
- [17] S. Bolognani, R. Carli, G. Cavraro, S. Zampieri, A distributed control strategy for optimal reactive power flow with power and voltage constraints, in: IEEE International Conference on Smart Grid Communications (SmartGridComm), 2013, pp. 115–120. doi:10.1109/SmartGridComm.2013.6687943.
- [18] E. Dall’Anese, H. Zhu, G. B. Giannakis, Distributed optimal power flow for smart microgrids, IEEE Trans. on Smart Grid 4 (3) (2013) 1464–1475.
- [19] B. Zhang, A. Lam, A. Dominguez-Garcia, D. Tse, An optimal and distributed method for voltage regulation in power distribution systems, IEEE Trans. on Power Systems PP (99) (2014) 1–13. doi:10.1109/TPWRS.2014.2347281.
- [20] M. Kraning, E. Chu, J. Lavaei, S. Boyd, Dynamic network energy management via proximal message passing, Foundations and Trends in Optimization 1 (2) (2013) 70–122.
- [21] A. X. Sun, D. T. Phan, S. Ghosh, Fully decentralized AC optimal power flow algorithms, in: Power and Energy Society General Meeting (PES), IEEE, 2013, pp. 1–5.
- [22] P. Sulc, S. Backhaus, M. Chertkov, Optimal distributed control of reactive power via the alternating direction method of multipliers, IEEE Trans. on Energy Conversion 29 (4) (2014) 968–977. doi:10.1109/TEC.2014.2363196.
- [23] Q. Peng, S. H. Low, Distributed algorithm for optimal power flow on a radial network, arXiv preprint arXiv:1404.0700.

- 510 [24] T. Erseghe, Distributed optimal power flow using ADMM, *IEEE Trans. on Power Systems* 29 (5) (2014) 2370–2380. doi:10.1109/TPWRS.2014.2306495.
- [25] A. G. Bakirtzis, P. N. Biskas, A decentralized solution to the DC-OPF of interconnected power systems, *IEEE Trans. on Power Systems* 18 (3) 515 (2003) 1007–1013.
- [26] B. Lesieutre, D. Molzahn, A. Borden, C. Demarco, Examining the limits of the application of semidefinite programming to power flow problems, in: 2011 49th Annual Allerton Conference on Communication, Control, and Computing (Allerton), 2011, pp. 1492–1499. doi:10.1109/Allerton. 520 2011.6120344.
- [27] D. P. Palomar, M. Chiang, A tutorial on decomposition methods for network utility maximization, *IEEE Journal on Selected Areas in Communications* 24 (8) (2006) 1439–1451.
- [28] A. J. Conejo, J. A. Aguado, Multi-area coordinated decentralized DC optimal power flow, *IEEE Trans. on Power Systems* 13 (4) (1998) 1272–1278. 525
- [29] P. N. Biskas, A. G. Bakirtzis, N. I. Macheras, N. K. Pasialis, A decentralized implementation of DC optimal power flow on a network of computers, *IEEE Trans. on Power Systems* 20 (1) (2005) 25–33.
- [30] O. Alsac, J. Bright, M. Prais, B. Stott, Further developments in LP-based 530 optimal power flow, *IEEE Trans. on Power Systems* 5 (3) (1990) 697–711.
- [31] B. Stott, O. Alsac, Fast decoupled load flow, *IEEE Trans. on Power Apparatus and Systems* (3) (1974) 859–869.
- [32] M. Baran, F. Wu, Optimal sizing of capacitors placed on a radial distribution system, *IEEE Trans. on Power Delivery* 4 (1) (1989) 735–743. 535 doi:10.1109/61.19266.

- [33] S. Bose, D. F. Gayme, K. M. Chandy, S. H. Low, Quadratically constrained quadratic programs on acyclic graphs with application to power flow, arXiv preprint arXiv:1203.5599.
- [34] L. Gan, S. Low, Convexification of AC optimal power flow, PSCC.
- 540 [35] R. A. Jabr, Radial distribution load flow using conic programming, IEEE Trans. on Power Systems 21 (3) (2006) 1458–1459.
- [36] J. Lavaei, S. Low, Zero duality gap in optimal power flow problem, IEEE Trans. on Power Systems 27 (1) (2012) 92–107. doi:10.1109/TPWRS.2011.2160974.
- 545 [37] M. Farivar, C. R. Clarke, S. H. Low, K. M. Chandy, Inverter VAR control for distribution systems with renewables, in: International Conference on Smart Grid Communications (SmartGridComm), IEEE, 2011, pp. 457–462.
- [38] B. Stott, J. Jardim, O. Alsac, DC power flow revisited, IEEE Trans. on Power Systems 24 (3) (2009) 1290–1300.
- 550 [39] W. Bukhsh, A. Grothey, K. McKinnon, P. Trodden, Local solutions of the optimal power flow problem, IEEE Trans. on Power Systems 28 (4) (2013) 4780–4788. doi:10.1109/TPWRS.2013.2274577.
- [40] M. Farivar, S. H. Low, Branch flow model: Relaxations and convexification., in: CDC, 2012, pp. 3672–3679.
- 555 [41] N. Li, L. Chen, S. H. Low, Exact convex relaxation of OPF for radial networks using branch flow model., in: SmartGridComm, Citeseer, 2012, pp. 7–12.
- [42] L. Gan, N. Li, U. Topcu, S. Low, Branch flow model for radial networks: convex relaxation, in: Proceedings of the 51st IEEE Conference on Decision and Control, 2012.
- 560 [43] R. Cespedes, New method for the analysis of distribution networks, IEEE Trans. on Power Delivery 5 (1) (1990) 391–396. doi:10.1109/61.107303.

- [44] H.-D. Chiang, M. Baran, On the existence and uniqueness of load flow solution for radial distribution power networks, IEEE Trans. on Circuits and Systems 37 (3) (1990) 410–416. doi:10.1109/31.52734.
- [45] S. Boyd, N. Parikh, E. Chu, B. Peleato, J. Eckstein, Distributed optimization and statistical learning via the alternating direction method of multipliers, Foundations and Trends® in Machine Learning 3 (1) (2011) 1–122.
- [46] W. D. Stevenson, J. J. Grainger, Power system analysis, New York: McGraw-Hill International Editions (1994) 141–190.

AC OPF in Radial Distribution Networks - Part II: An Augmented Lagrangian-based OPF Algorithm, Distributable via Primal Decomposition

Konstantina Christakou^{a,b}, Dan-Cristian Tomozei^c, Jean-Yves Le Boudec^a,
Mario Paolone^{b,*}

^a*Laboratory for Communications and Applications 2, Ecole Polytechnique Fédérale de
Lausanne, CH-1015 Lausanne, Switzerland*

^b*Distributed Electrical Systems Laboratory, Ecole Polytechnique Fédérale de Lausanne,
CH-1015 Lausanne, Switzerland*

^c*Cisco Systems, Inc, EPFL Innovation Park Building E 1015 Lausanne, Switzerland*

Abstract

In the first part of this two-part paper we show that the branch-flow convexification of the OPF problem is not exact and that the ADMM-based decomposition of the OPF fails to converge in specific scenarios. Therefore, there is a need to develop algorithms for the solution of the non-approximated OPF problem that remains inherently non-convex. To overcome the limitations of recent approaches for the solution of the OPF problem, we propose in this paper, a specific algorithm for the solution of a non-approximated, non-convex AC OPF problem in radial distribution systems. It is based on the method of multipliers, as well as on a primal decomposition of the OPF problem. We provide a centralized version, as well as a distributed asynchronous version of the algorithm. We show that the centralized OPF algorithm converges to a local minimum of the global OPF problem and that the distributed version of the algorithm converges to the same solution as the centralized one. Here, in this second part of the two-part paper, we provide the formulation of the proposed algorithm and we evaluate its performance by using both small-scale electrical networks,

*Corresponding author. Phone number: +41 21 69 32662, Postal address: EPFL STI IEL
DESL ELL 136 (Bâtiment ELL), Station 11, CH-1015 Lausanne

Email addresses: konstantina.christakou@epfl.ch (Konstantina Christakou),
dtomozei@cisco.com (Dan-Cristian Tomozei), jean-yves.leboudec@epfl.ch (Jean-Yves Le
Boudec), mario.paolone@epfl.ch (Mario Paolone)

as well as a modified IEEE 13-node test feeder.

Keywords: OPF, ADMM, decomposition methods, method of multipliers, convex relaxation, active distribution networks, distributed algorithms, asynchronous algorithms.

1. Introduction

In Part I of this two-part paper we present the generic formulation of the non-convex OPF problem and we briefly review several OPF algorithms that are based on approximations and assumptions in order to guarantee convergence. Furthermore, we focus on the branch-flow convexification of the OPF problem that has been recently proposed by Farivar and Low in [1, 2] and is claimed to be exact for the case of radial distribution systems under specific assumptions, despite the absence of apparent approximations. We show that this claim, in fact, does not hold, as it leads to an incorrect system model and therefore, there is a need to develop algorithms for the solution of the non-approximated OPF problem that remains inherently non-convex. In detail, we show through practical examples that in [1, 2], on one hand, there is a misinterpretation of the physical network model related to the ampacity constraint of the lines' current flows and, on the other hand, the proof of the exactness of the proposed relaxation requires unrealistic assumptions related to the unboundedness of specific control variables. Furthermore, we investigate the application of ADMM for the solution of the original non-approximated OPF problem. Even though ADMM requires the underlying problem to be convex in order to guarantee convergence, it was applied also to the case of non-convex AC OPF problems with promising convergence performance (e.g., [3, 4]). However, we show, through practical examples, cases for which the ADMM-based decomposition of the non-relaxed OPF problem fails to converge.

To overcome the aforementioned limitations, here in this second part, we propose an algorithm for the solution of the non-approximated non-convex AC OPF problem in radial networks. Our proposed solution uses an augmented

Lagrangian approach and relies on the method of multipliers ([5, 6, 7]). In particular, we design a centralized OPF algorithm that is proven to converge to a local minimum of the original non-approximated OPF problem.

With respect to the case of controlling multiple dispersed energy resources,
 30 it is of interest to also define a distributed solution method that is formally equivalent to the centralized formulation. In fact, several distributed OPF algorithms are proposed in the literature. In [8, 9] the authors design a dual-ascent algorithm for optimal reactive power flow with power and voltage constraints. In [10, 11] dual decomposition is used as the basis for the distributed solution
 35 of the OPF problem. Finally, a significant number of contributions propose distributed formulations of the OPF problem, based on the alternating direction method of multipliers (ADMM) (e.g., [12, 10, 3, 13, 14, 4]).

In this direction, we present, here in this second part, a distributed version of the proposed algorithm that, unlike ADMM, is based on a primal decomposition
 40 tion [15] and does not require that the problem be convex. In this decentralized version of the algorithm, at each iteration, local agents, assigned to network buses and network lines, exchange messages with their neighbors using only local information. We prove that the distributed algorithm converges to the same solution as the centralized version. Finally, we present an asynchronous imple-
 45 mentation of the distributed algorithm where the messages of the neighboring agents need not be synchronized.

The structure of this second part is the following. In Section II we describe the proposed algorithm for the OPF solution. We present both a centralized, as well as a decentralized asynchronous version of the proposed algorithm. In
 50 Section III we investigate the convergence of the proposed algorithm in the cases where the BFM convexification leads to an incorrect solution and ADMM fails to converge to a solution. In Section IV we evaluate the performance of the proposed algorithm using a modified IEEE 13-node test feeder. Finally, in Section V we provide the main observations and concluding remarks for this
 55 Part II.

2. AC OPF in Radial Distribution Systems

We first write the AC OPF problem presented in Part I in an equivalent form, and then we provide a centralized, as well as a distributed algorithm for its resolution.

60 We make the following assumptions about the grid model:

- A1. We consider a direct sequence representation of the grid;
- A2. Any two-port component (e.g., lines, transformers etc.) is represented as a π -equivalent;
- A3. We assume a perfect knowledge of the system parameters, i.e., the network
65 admittance matrix is known;
- A4. The nodal-power injections are voltage-independent;
- A5. The control variables are composed by the nodal power injections/absorptions.

2.1. The Proposed Centralized OPF Algorithm

We are interested in maximizing the social welfare of the economic agents
70 that use the grid, while maintaining an acceptable network voltage profile and respecting the line ampacity limits. Specifically, we tune the line ampacities and the network voltage profiles by controlling the (P, Q) -injections of distributed controllable devices \mathcal{G} (e.g., renewable generators) in a “fair” way: Each controllable device $g \in \mathcal{G}$ has a certain utility function $U_g(\cdot)$, and the sum of
75 these utility functions is maximized subject to the satisfaction of the network operation constraints (voltage and ampacity). The resulting set-point is thus Pareto-optimal, i.e., no single device can increase its utility without hurting the utility of some other device, and locally-“fair”, i.e., the resulting set-point is a local maximizer of the sum of the device utilities lying on the Pareto boundary
80 of feasible set-points.

By convention, each line $\ell \in \mathcal{L}$ has a “receiving” and a “sending” end, which we denote by ℓ^+ and ℓ^- , respectively. These are chosen arbitrarily. A line is connected to two adjacent buses to which we refer by $\beta(\ell^+)$ and $\beta(\ell^-)$, respectively. For each line, we introduce two auxiliary variables \bar{E}_{ℓ^+} and \bar{E}_{ℓ^-} representing

the complex voltage at the two ends of the line. Assumptions A1-A3 allow us to express the corresponding injected currents and powers at the two ends of line ℓ :

$$\bar{I}_{\ell+} = \bar{I}_{\ell+}(\bar{E}_{\ell+}, \bar{E}_{\ell-}) = (\bar{Y}_{\ell} + \bar{Y}_{\ell_0^+})\bar{E}_{\ell+} - \bar{Y}_{\ell}\bar{E}_{\ell-} \quad (1)$$

$$\bar{I}_{\ell-} = \bar{I}_{\ell-}(\bar{E}_{\ell+}, \bar{E}_{\ell-}) = (\bar{Y}_{\ell} + \bar{Y}_{\ell_0^-})\bar{E}_{\ell-} - \bar{Y}_{\ell}\bar{E}_{\ell+} \quad (2)$$

$$\bar{S}_{\ell+} = \bar{S}_{\ell+}(\bar{E}_{\ell+}, \bar{E}_{\ell-}) = \bar{E}_{\ell+}\bar{I}_{\ell+} \quad (3)$$

$$\bar{S}_{\ell-} = \bar{S}_{\ell-}(\bar{E}_{\ell+}, \bar{E}_{\ell-}) = \bar{E}_{\ell-}\bar{I}_{\ell-} \quad (4)$$

In the remainder of this paper, unless otherwise stated, the complex line currents and powers expressed above are always computed according to equations (1)-(4). They are thus all functions of $\bar{E}_{\ell+}$ and $\bar{E}_{\ell-}$ *exclusively*, although the arguments are often omitted for the sake of brevity. All quantities are expressed in “per-unit”, unless otherwise specified. 85

For readability, we denote the vector formed by the real and imaginary parts of variables $(\bar{E}_{\ell+}, \bar{E}_{\ell-})_{\ell}$ by $y \in \mathbb{R}^{4L}$, where $L = |\mathcal{L}|$ is the number of lines. Note that for a given value of y , the corresponding currents and powers do not necessarily satisfy Kirchhoff's law.

We call y feasible if it satisfies voltage consistency and per-bus power-balance. Voltage consistency means that the voltages of all the lines incident to a specific bus $b \in \mathcal{B}$ are identical, *i.e.*, have the same amplitude V_b and the same argument φ_b :

$$|\bar{E}_{\ell+}| = V_{\beta(\ell+)}, \quad |\bar{E}_{\ell-}| = V_{\beta(\ell-)} \quad (5)$$

$$\arg(\bar{E}_{\ell+}) = \varphi_{\beta(\ell+)}, \quad \arg(\bar{E}_{\ell-}) = \varphi_{\beta(\ell-)}, \quad \forall \ell \in \mathcal{L}. \quad (6)$$

At each bus $b \in \mathcal{B}$, power-balance is satisfied if and only if

$$\sum_{\beta(\ell^+)=b} \bar{S}_{\ell+} + \sum_{\beta(\ell^-)=b} \bar{S}_{\ell-} = - \sum_{g \in b} \bar{S}_g - \bar{S}(b), \quad \forall b \in \mathcal{B}, \quad (7)$$

where S_g is the controlled generated power of device g found at bus b , $\bar{S}(b)$ denotes the non-controllable power injection at bus b , and $\bar{S}_{\ell+}$, $\bar{S}_{\ell-}$ are obtained via (3)-(4). 90

If y is feasible, it is important to note that equations (1)-(4) describe the exact AC power-flow equations. Hence, we use a non-approximated model of
 95 the grid.

We write the OPF formulation (Part I) equivalently:¹

$$\max_{\substack{\bar{S}_g, V_b, \varphi_b \\ \bar{E}_{\ell+}, \bar{E}_{\ell-}}} \sum_{g \in \mathcal{G}} W_g(\bar{S}_g) \quad \text{subject to:} \quad (8)$$

Feasibility constraints (5), (6), (7)

$$|\bar{I}_{\ell+}| \leq I_{\ell, \max} \text{ and } |\bar{I}_{\ell-}| \leq I_{\ell, \max}, \quad \forall \ell \in \mathcal{L} \quad (9)$$

$$V_{\min} \leq V_b \leq V_{\max}, \quad \forall b \in \mathcal{B} \quad (10)$$

$$\bar{S}_g \in \mathcal{H}_g, \quad \forall g \in \mathcal{G} \quad (11)$$

As previously stated, the objective function is the sum of the welfare of the controllable devices W_g . In the above formulation, we denote by \mathcal{G} the set of controllable devices and by $\bar{S}_g = P_g + jQ_g$ the controllable injected power by device g , subject to the capability constraint (11). The set \mathcal{G} can contain both generators and consumers. However, for the sake of presentation clarity, we consider that \mathcal{G} contains uniquely PV generators. This is not a limiting assumption, as our results apply to any device with controllable power injections (including controllable loads). Non-controllable loads do not appear in the objective function, that expresses the utility of PV generators (a concave increasing function $U(\cdot)$ of active power injection) and the losses of the power converter:

$$W_g(\bar{S}_g) = U_g(P_g) - \eta(P_g^2 + Q_g^2), \quad \forall g \in \mathcal{G}. \quad (12)$$

We consider typical capability curves of PV power inverters:

$$\mathcal{H}_g = \{\bar{S}_g : |\bar{S}_g| \leq S_{g, \max}, \quad |\arg(\bar{S}_g)| \leq \phi_{g, \max}\}. \quad (13)$$

In order to solve the problem (8)-(11), we convert the inequality constraints

¹Unlike in Part I, we consider wlog that there are two types of connected devices: they either have controllable power injection \bar{S}_g or impose an overall fixed power injection $\bar{S}(b)$ in bus b .

(9) to equality constraints by introducing slack variables $i_{\ell+}$ and $i_{\ell-}$ as follows:

$$|\bar{I}_{\ell+}| + i_{\ell+} = I_{\ell,\max} \text{ and } |\bar{I}_{\ell-}| + i_{\ell-} = I_{\ell,\max}, \forall \ell \in \mathcal{L} \quad (14)$$

$$i_{\ell+}, i_{\ell-} \geq 0, \quad \forall \ell \in \mathcal{L} \quad (15)$$

We denote by x the real vector of variables formed by the artificial control variables $(V_b, \varphi_b)_{b \in \mathcal{B}}$, $(i_{\ell+}, i_{\ell-})_{\ell \in \mathcal{L}}$, and the device controllable injected power $(P_g, Q_g)_{g \in \mathcal{G}}$.

Notice that all the equality constraints above, (5), (6), (7), and (14) can be summarized as $g(y) + Ax + b = 0$, where $g(\cdot)$ is a smooth non-convex function that can be derived from equations (1)-(6), and A is a positive definite matrix. Similarly, the inequality constraints, (10), (11), and (15), can be expressed as $h(x) \geq 0$, where $h(x)$ is a convex function that can be derived from equations (10), (15), and (13). We denote the objective by $f(x)$, where f is concave.

We can thus write our problem in the more compact form:

$$\max_{x,y} f(x) \quad (16)$$

$$\text{subject to } g(y) + Ax + b = 0 \quad (17)$$

$$h(x) \geq 0. \quad (18)$$

We write its augmented Lagrangian ([5, 6, 7]):

$$\begin{aligned} \mathcal{L}_\rho(x, y; \lambda) = & f(x) + \lambda'(g(y) + Ax + b) \\ & - \frac{\rho}{2} \|g(y) + Ax + b\|^2, \end{aligned} \quad (19)$$

where ρ is the weight of the quadratic penalty term added to the classic Lagrangian function, and λ is the vector of Lagrange multipliers associated with the equality constraints (17).

Our centralized iterative algorithm for solving the OPF is based on the method of multipliers ([5, §4.2]). This method was first introduced for solving iteratively non-linear equality constrained problems. It is shown to converge under more general conditions than dual ascent [16]. Algorithm 1 summarizes the proposed centralized algorithm, and Theorem 1 characterizes its convergence.

The main advantage of the method of multipliers is that there exists a finite
 115 value $\bar{\rho}$ such that the problem (20) is locally convex for all $\rho^k > \bar{\rho}$. Note also
 that the algorithm bounds the value of λ at each iteration. The next vector of
 multiplier estimates λ is obtained after a projection on the set $[-\bar{\lambda}, \bar{\lambda}]$ defined as
 $[-\bar{\lambda}_1, \bar{\lambda}_1] \times [-\bar{\lambda}_2, \bar{\lambda}_2] \times \dots$; the constant vector $\bar{\lambda}$ is chosen such that the sought
 optimal vector of Lagrange multipliers λ^* lies in $[-\bar{\lambda}, \bar{\lambda}]$ (see [17, §2.2.2]).

120 **Theorem 1.** *For smooth objective function $f \in \mathcal{C}^2$ and suitably chosen $\bar{\lambda}$ such
 that the optimal vector of Lagrange multipliers λ^* satisfies $\lambda^* \in [-\bar{\lambda}, \bar{\lambda}]$, Algo-
 rithm 1 converges to a local minimum of the nonlinear program (16)-(18).*

Proof. By [17, Proposition 1.23], our problem satisfies assumption (S) from [17,
 §2.2], since the equality constraint is a \mathcal{C}^2 function of y , and the objective func-

Algorithm 1 Centralized algorithm for the OPF (16)-(18)

- Set $k=0$ and initialize control variables x and y :
 $\bar{S}_g^0 = 0, \bar{E}_{\ell+}^0 = \bar{E}_{\ell-}^0 = 1, V_b^0 = 1, \varphi_b^0 = 0, i_{\ell+}^0 = i_{\ell-}^0 = 0$ (per-unit),
 Lagrange multipliers $\lambda^0 = 0$, increasing gain sequence $(\rho^k)_k, \rho^k \rightarrow \infty$.

1: **repeat**

2: Maximize the augmented Lagrangian for fixed $\lambda = \lambda^k$:

$$(x^{k+1}, y^{k+1}) = \arg \max_{x, y: h(x) \geq 0} L_{\rho^k}(x, y; \lambda^k). \quad (20)$$

3: Update the Lagrange multipliers:

$$\lambda^{k+1} = \Pi_{[-\bar{\lambda}, \bar{\lambda}]} \{ \lambda^k + \rho^k [g(y^{k+1}) + Ax^{k+1} + b] \} \quad (21)$$

4: $k \leftarrow k+1$

5: **until** the maximum number of iterations has been reached **or** the change
 in the Lagrange multipliers between two consecutive iterations is less than
 a tolerance $\delta > 0$

tion is chosen to be \mathcal{C}^2 . Proposition 2.7 from the same reference guarantees the desired convergence, if the iterates (x^k, y^k, λ^k) reach the set D from Proposition 2.4 of [17], *i.e.*, if there exists a \bar{k} such that $(x^{\bar{k}}, y^{\bar{k}}, \lambda^{\bar{k}}) \in D$ (for all the following indices $k > \bar{k}$, the iterates stay in D , and convergence ensues). The existence of such a \bar{k} follows from the choice of the divergent increasing sequence of gains (ρ^k) and from the boundedness of the sequence (λ^k) . \square

Due to the quadratic terms in the expression of the augmented Lagrangian (19), the optimization problem in (20) does not decouple across the network and, therefore, cannot be solved in a distributed manner. In the following section, we reformulate this problem in an equivalent way that leads to a distributed algorithm for its resolution.

2.2. Distributed Solution of the OPF Problem

We adopt a primal decomposition method [15] that gives an iterative algorithm for the minimization of the problem in *Step 2* of Algorithm 1. In (19) the line voltages $y = (\bar{E}_{\ell+}, \bar{E}_{\ell-})$ are “coupling” variables. If these variables are fixed to a specific value, then problem (20) decouples in smaller, easier (convex) problems, that can be solved by local agents.

Specifically, to solve (20) iteratively for fixed values of the Lagrange multiplier estimates $\hat{\lambda}$ and fixed gain $\hat{\rho}$ we take the following approach: At the n -th iteration, the value of the coupling variables $y^n = (\bar{E}_{\ell+}^n, \bar{E}_{\ell-}^n)$ is assumed fixed. The x variables, *i.e.*, the power set-points of the controllable devices (\bar{S}_g) , the bus voltages (\bar{V}_b) , and the slack variables $i_{\ell+}, i_{\ell-}$, are computed by solving the following constrained convex optimization problem:

$$x^{n+1} = \arg \max_{x: h(x) \geq 0} L_{\hat{\rho}}(x, y^n, \hat{\lambda}). \quad (22)$$

Next, the coupling variables y are updated as follows:

$$y^{n+1} = y^n + \alpha^n (\nabla_y L_{\hat{\rho}})(x^{n+1}, y^n, \hat{\lambda}), \quad (23)$$

where α^n is a positive step-size sequence of the gradient descent. The choice of the step-size is related to the topology of the network and the parameters of the lines (i.e., the network admittance matrix). For example, a large constant
150 step-size might not allow the algorithm to converge, whereas a small constant step-size could cause slow convergence².

The algorithm stops when the norm of the update in the y variables is less than some small positive tolerance ε , i.e., when $\|\nabla_y L_{\hat{\rho}}(x^{n+1}, y^n, \hat{\lambda})\| \leq \varepsilon$.

155 **Theorem 2.** *The algorithm (22)-(23) with tolerance ε in the stopping criterion converges to a vicinity $\mathcal{B}((x^*, y^*), \delta)$ of a local optimum (x^*, y^*) of problem (20). If (20) is strongly locally convex in y in a vicinity of (x^*, y^*) , then $\delta = \Theta(\varepsilon^2)$.*

Proof. (Sketch) Denote $v(y) = \max_{x: h(x) \geq 0} L_{\hat{\rho}}(x, y, \hat{\lambda})$ and $x^*(y)$ the value of x that achieves this maximum (22). Theorem 2.1 of [18] says that the optimum
160 $(x^*(y^*), y^*)$ of $\max_y v(y)$ coincides with the one of (20). Moreover, a δ -optimal solution $(x^*(y_\delta), y_\delta)$ of $\max_y v(y)$ (that is, $v(y_\delta) \geq v(y^*) - \delta$) is also δ -optimal for (20).

We now show that it holds that $\nabla_y v(y) = (\nabla_y L_{\hat{\rho}})(x^*(y), y, \hat{\lambda})$, or equivalently, $\frac{Dx^*(y)}{Dy}(\nabla_x L_{\hat{\rho}})(x^*(y), y, \hat{\lambda}) = 0$. If we can show this, then the algorithm
165 (22)-(23) is equivalent to a gradient ascent in y on $v(y)$. It is easy to show that the function $v(y)$ is “smooth” (\mathcal{C}^2). By the strong local convexity around (x^*, y^*) of the augmented Lagrangian, [5, Exercise 1.2.10] allows us to conclude that $\delta = \Theta(\varepsilon^2)$.

Note that problem (22) is convex. Consider the optimal multipliers μ^* corresponding to the constraints $h(x) \geq 0$. They satisfy the KKT conditions:

$$\begin{aligned} (\nabla_x L_{\hat{\rho}})(x^*(y), y, \hat{\lambda}) &= \sum_i \mu_i^*(y) \nabla_x h_i(x^*(y)) \\ \mu_i^*(y) h_i(x^*(y)) &= 0; \quad \mu_i^* \geq 0. \end{aligned}$$

Define the following functions: $\psi_i(y) := h_i(x^*(y))$. Since $x^*(y)$ is always feasible,

²In order to properly tune this parameter, a dedicated off-line study can be performed before deployment of the proposed algorithm.

it means that $\psi_i(y) \geq 0$. Consider the set of indices $\mathcal{I}_0(y) := \{i : h_i(x^*(y)) = 0\}$. Take some $i \in \mathcal{I}_0(y)$. In this case the function $\psi_i(y)$ has an extremal point in y , which implies that $\nabla_y \psi_i(y) = 0$, or again that $\frac{Dx^*(y)}{Dy} \nabla_x h_i(x^*(y)) = 0$. For all $i \notin \mathcal{I}_0(y)$, by KKT we have $\mu_i^*(y) = 0$. By the above arguments,

$$\begin{aligned} & \frac{Dx^*(y)}{Dy} (\nabla_x L_{\hat{\rho}})(x^*(y), y, \hat{\lambda}) \\ &= \sum_i \mu_i^*(y) \frac{Dx^*(y)}{Dy} \nabla_x h_i(x^*(y)) = 0. \end{aligned}$$

□

Thanks to its separability property, problem (22) can be solved in a distributed manner. Bus agents can be responsible for updating the power set-points of the controllable devices (\bar{S}_g) that are connected to them, as well as their voltages (\bar{V}_b) in parallel, and lines can be responsible for updating the slack variables ($i_{\ell+}, i_{\ell-}$). Specifically, the ‘power set-points (\bar{S}_g^{n+1}) of devices in bus b are obtained by solving the following convex problem:

$$\begin{aligned} (\bar{S}_g^{n+1}) &= \arg \max_{\bar{S}_g \in \mathcal{H}_g} \sum_{g \in b} W_g(\bar{S}_g) \\ &\quad - \frac{\hat{\rho}}{2} \left| \sum_{g \in b} \bar{S}_g + \bar{S}(b) + \sum_{\beta(\ell^+) = b} \bar{S}_{\ell^+}^n + \sum_{\beta(\ell^-) = b} \bar{S}_{\ell^-}^n - \frac{\hat{\lambda}_b}{\hat{\rho}} \right|^2, \end{aligned}$$

170 where $\hat{\lambda}_b$ is the given multiplier corresponding to the constraint (7) of bus b . The other problems (for the other x variables) have simpler expressions that we do not reproduce for brevity sake.

Similarly, (23) can be decomposed across the different network lines: line-
agents can update the voltages at their two ends in parallel. In terms of required
175 information, each bus agent needs to know only the voltage values of the lines that are incident to it, the constraints of the devices, and the state of the loads that are connected to it. Finally, in order to compute the partial derivatives of (23) with respect to its voltages, each line requires solely the information of the power balance and the voltage values of its two adjacent buses. The actual
180 implementation of the distributed synchronous OPF algorithm is summarized below in Algorithm 2.

Theorem 3. For smooth objective function $f \in \mathcal{C}^2$ and suitably chosen $\bar{\lambda}$ such that the optimal vector of Lagrange multipliers λ^* satisfies $\lambda^* \in [-\bar{\lambda}, \bar{\lambda}]$, Algorithm 2 converges to a local minimum of the nonlinear program (16).

185 *Proof.* The proof is similar to the one of Theorem 1. It uses Proposition 2.16 of [17] for convergence, which only requires at each iteration a δ^k -optimal solution for (20) with $\delta^k \rightarrow 0$. By Theorem 2 we can conclude. \square

In a realistic setting, in order to take full advantage of the distributed formulation of the OPF algorithm, as described above and to avoid the overhead
190 cost of coordination between agents, the updates should be performed in an asynchronous fashion. Contrary to ADMM-based algorithms, which require a

Algorithm 2 Distributed algorithm for the OPF (16)-(18)

- Set $k=0$ and initialize control variables x and y :
 $\bar{S}_g^0 = 0, \bar{E}_{\ell+}^0 = \bar{E}_{\ell-}^0 = 1, V_b^0 = 1, \varphi_b^0 = 0, i_{\ell+}^0 = i_{\ell-}^0 = 0$ (per-unit),
 Lagrange multipliers $\lambda^0 = 0$, increasing diverging gain sequence $(\rho^k)_k$,
 $\rho^k \rightarrow \infty$, decreasing tolerance sequence $(\varepsilon^k \geq 0)_k, \varepsilon^k \rightarrow 0$.
 - 1: **repeat**
 - 2: $n \leftarrow 0; \tilde{x}^0 \leftarrow x^k; \tilde{y}^0 \leftarrow y^k$
 - 3: **repeat**
 - 4: $\tilde{x}^{n+1} = \arg \max_{x: h(x) \geq 0} L_{\rho^k}(x, \tilde{y}^n, \lambda^k)$
 - 5: $\tilde{y}^{n+1} = \tilde{y}^n + \alpha^n (\nabla_y L_{\rho^k})(\tilde{x}^{n+1}, \tilde{y}^n, \lambda^k)$
 - 6: $n \leftarrow n+1$
 - 7: **until** $\|\nabla_y L_{\rho^k}(\tilde{x}^{n+1}, \tilde{y}^n, \lambda^k)\| \leq \varepsilon^k$
 - 8: $x^{k+1} \leftarrow \tilde{x}^{n+1}; y^{k+1} \leftarrow \tilde{y}^{n+1}$
 - 9: $\lambda^{k+1} = \Pi_{[-\bar{\lambda}, \bar{\lambda}]} \{ \lambda^k + \rho^k [g(y^{k+1}) + Ax^{k+1} + b] \}$
 - 10: $k \leftarrow k+1$
 - 11: **until** the maximum number of iterations has been reached **or** the change in the Lagrange multipliers between two consecutive iterations is less than a tolerance $\delta > 0$
-

synchronized implementation of the updates, the proposed algorithm can be implemented in an asynchronous manner. In this direction, we assume that each of the bus and line agents has its own two local poisson clocks with different rates. The clock with the lower rate ($C1$) triggers the multiplier update (21) and the clock with the higher rate ($C2$) triggers the events described in steps (22)-(23).

In detail, all the control variables and the Lagrange multipliers are first initialized. Then, every time the $C2$ clock of a bus ticks, this bus performs local update operations by using the most recent stored values for the voltages of its incident lines and for the associated Lagrange multipliers. Once the bus updates its power and voltage values, it informs the incident lines of the changes. Similarly, when the $C2$ clock of a line ticks, the line agent updates the variables $(i_{\ell+}, i_{\ell-})$ by taking into account the most recent values of the line current flows and associated Lagrange multipliers. In addition to this update, the updates of the voltages of its two end-points are triggered. In order to compute the new values, the line uses the most recent stored values for the adjacent buses' powers and voltages, and once the updates are completed the line communicates this information to its neighboring buses. Now, when the $C1$ clock of a bus or a line ticks, then the corresponding agent updates the Lagrange multipliers (21). It is worth noting, that we no longer have a serial implementation of the various updates like the ones presented in Algorithm 2. On the contrary, the different rates of the clocks are chosen in such a way to ensure that, on average, a sufficient number of the updates occurs before an update of the corresponding Lagrange multiplier takes place.

In this section, we investigate the performances and convergence properties of the centralized Algorithm 1 in several different scenarios. In particular, we consider the cases presented in Part I of the paper, where the BFM convexification leads to an incorrect solution of the OPF problem and ADMM fails to converge to a solution. Additionally, we investigate the performances of the proposed centralized algorithm under different initial conditions of the electrical-network state. In order to do so, we consider the same 4-bus test network that

was used in Part I of the paper. We assume a first test case where the controllable device connected to bus 4 is a generator, whereas controllable loads are connected to buses 2 and 3. The network characteristics, the base values, the capability limits of the controllable resources, and the voltage and ampacity limits are given in Part I (Fig. 3 and Table 7). In what follows, the objective function accounts for the minimization of the network losses, as well as for the utility of the generating units, namely:

$$\min_{\bar{S}_g, \bar{S}_\ell, V_b, \varphi_b, |\bar{I}_\ell|} - \sum_{g \in \mathcal{G}} \text{Re}(\bar{S}_g) + \sum_{\ell \in \mathcal{L}} \text{Re}(\bar{Y}_\ell) |\bar{I}_\ell|^2 \quad (24)$$

2.3. Effect of the Line Length, Network Rated Value and Network State on the Convergence of Algorithm 1

In order to compare the performances of the proposed algorithm with the OPF algorithm proposed in [1, 2], we solve the OPF problem for various line
220 lengths and network voltage rated values as in Part I of the paper. In particular, we assume that the line lengths are uniformly multiplied by a factor in the range $[1.25 - 7.5]$ (while keeping the network voltage rated value to its nominal value) and the network voltage rated value varies in the range $[15 - 40]kV$ (while keeping the line lengths to their nominal values). The evolution of the bus
225 voltages, the line-current flows, as well as the active and reactive powers, are shown in Figures 1-6. It is worth noting that in all the cases the proposed algorithm converges in a few iterations. Furthermore, we observe from Fig. 2 and Fig. 5 that the line-current flows satisfy the line ampacity limit, once the algorithm has converged, in all cases. In particular, in Fig. 2 it is worth observing
230 that as the line length increases the receiving and sending-end current flows of the same line become significantly different. The behavior of the current flows as the voltage rated value increases is similar (Fig. 5). This effect is due to the increasing contribution of the current flow toward the shunt elements of the lines. In fact, we show, in Figures 7 and 8, the amount of reactive power
235 produced by the shunt elements of the lines for the various values of the line lengths and the network voltage rated values. We observe that as the line length

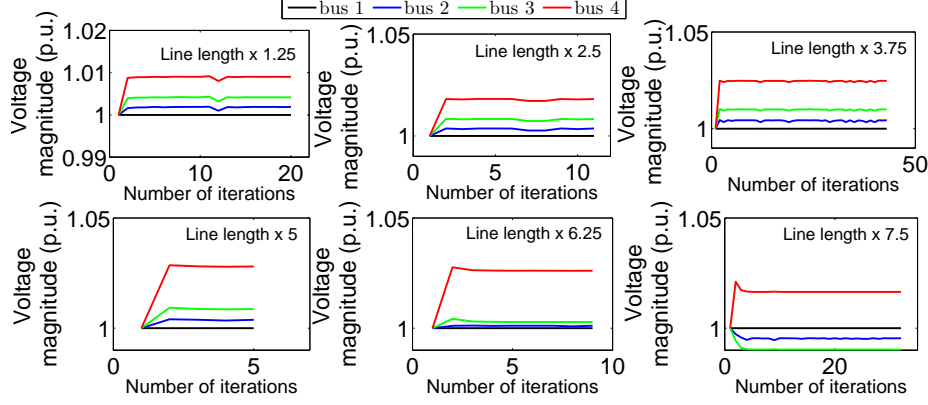


Fig. 1: Evolution of the magnitude of network voltages for various line lengths.

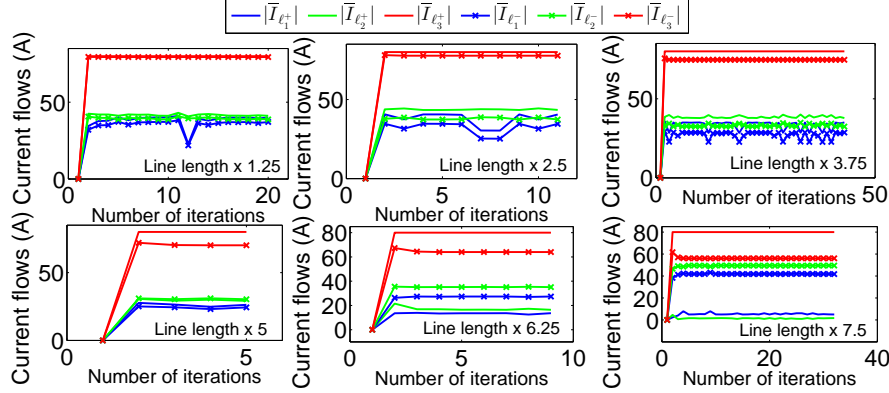


Fig. 2: Evolution of the line current flows for various line lengths.

increases or the rated value of the voltage increases the reactive power produced by the shunt elements of the line increases as well.

We investigate, in addition to the effect of the line lengths and the network
240 voltage rated value, the performance of the proposed algorithm under a different
network operating point. To this end, we consider a second test-case where the
controllable device connected to bus 4 is a controllable load and generators are
connected to buses 2 and 3. In this respect, we consider an extra term in the
objective function, which represents the utility associated with the controllable
245 load and is given by $(P_L - P_o)^2$, where P_o represents a constant amount of load
that has to be served. The capability limits of the controllable resources are

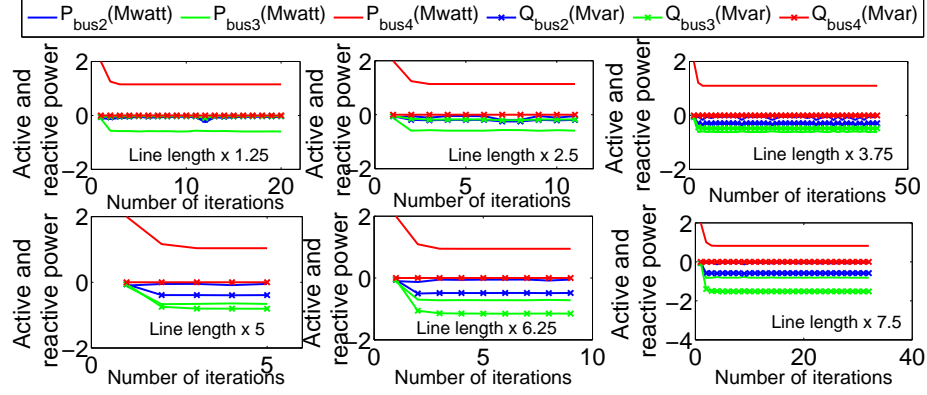


Fig. 3: Evolution of the active and reactive power of the controllable devices for various line lengths.

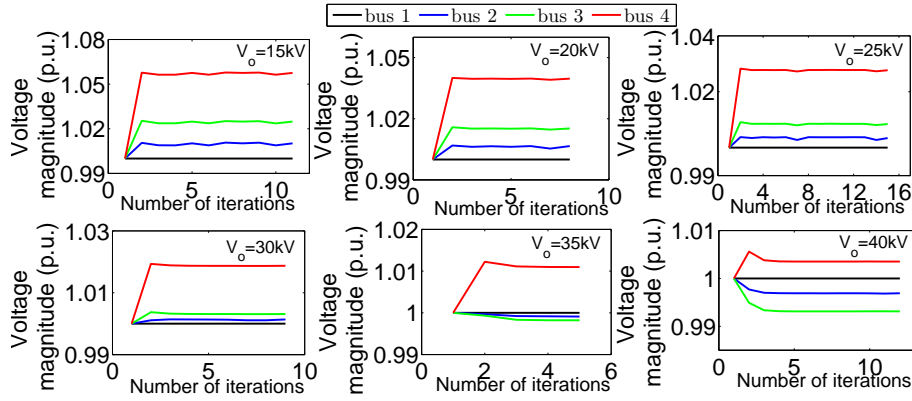


Fig. 4: Evolution of the magnitude of network voltages for various values of the network rated voltage.

shown in Table 1. The convergence of the voltages, current flows, as well as active and reactive powers are shown in Fig. 9. For the sake of brevity, we only show the evolution of the active and reactive power of the controllable load of bus 4, as the controllable generators are small and reach their maximum value upon convergence.

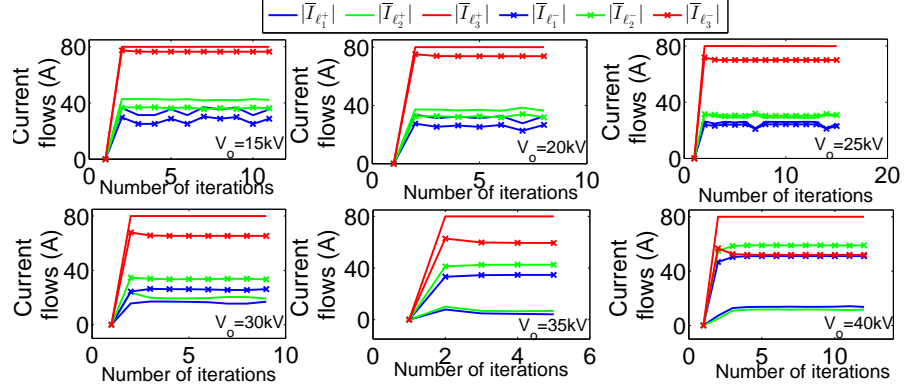


Fig. 5: Evolution of the line current flows for various values of the network rated voltage.

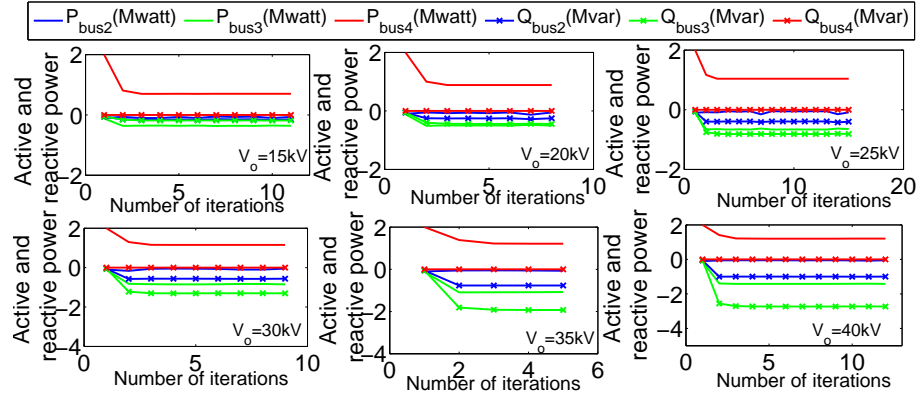


Fig. 6: Evolution of the magnitude of active and reactive power of the controllable devices for various values of the network rated voltage.

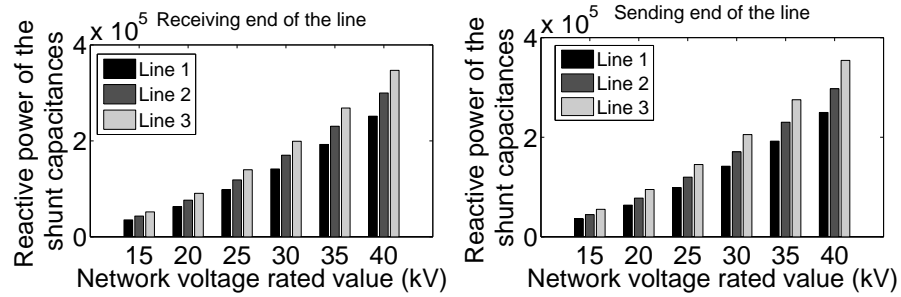


Fig. 7: Reactive power produced by the shunt elements of the lines for various values of the network voltage rated value.

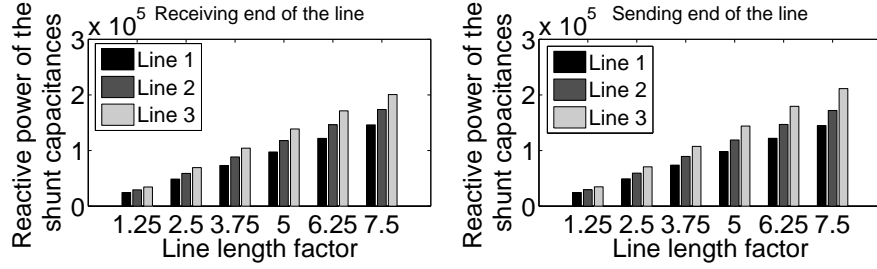


Fig. 8: Reactive power produced by the shunt elements of the lines for various line lengths.

Table 1: Parameters of the test network used for the investigation of the performance of the proposed OPF algorithm under a different operating point

Parameter	value
$[P_{g_{min}}, P_{g_{max}}](\text{bus } 2) \text{ (MW)}$	$[0, 0.01]$
$[P_{g_{min}}, P_{g_{max}}](\text{bus } 3) \text{ (MW)}$	$[0, 0.012]$
$(P_{c_{min}}, Q_{c_{min}})(\text{MW, Mvar}) \text{ (bus } 4)$	$0.3, 0.15$
$P_o(\text{MW}) \text{ (bus } 4)$	1

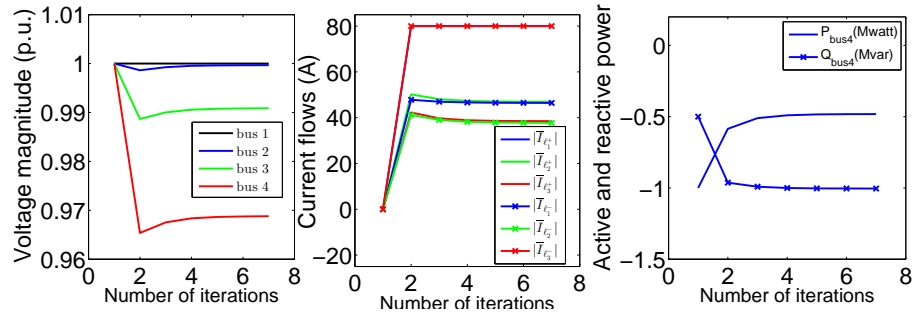


Fig. 9: Evolution of the magnitude of network voltages, current flows, as well as active and reactive power of the controllable load at bus 4 for the case of low generation and high load in the network.

Table 2: Parameters of the test network used for the evaluation of Algorithm 1 in the presence of shunt capacitors in the network

Parameter	Value
Generators' power, $ \bar{S}_{i_{gmax}} , i = 2, 3, 4$ (MVA)	0.40, 0.39, 0.46
Generators' power factor, $\cos\phi_{i_g}, i = 2, 3, 4$	0.9
Loads' active power, $P_{i_c}, i = 2, 3, 4$ (MW)	2.76, 2.16, 2.46
Loads' reactive power, $Q_{i_c}, i = 2, 3, 4$ (MW)	1.38, 1.08, 1.23
Shunt capacitor (bus 2)(uF)	859
Penalty term gain, ρ	10^4
Tolerance and maximum number of iterations	$10^{-4}, 10^4$
$[V_{min}, V_{max}]$ (p.u)	$[0.9, 1.1]$

2.4. Performance Evaluation of the Proposed Algorithm in the Presence of Shunt Capacitors in the Network

In what follows, we consider the same network adopted in the previous section and a case where each network bus, apart from the slack, has a load and a generator connected to it. The demand in the network is assumed to be non-controllable, whereas the generators are assumed to be distributed solar panels with typical PV-type capability constraints given by (13). For this scenario, the capability limits and the values of loads and generation are shown in Table 2.

In addition to the loads and generation, we consider that a shunt capacitor is connected to bus 2. In order to model this shunt capacitor, we consider that it is part of the first line. In particular, we consider that the shunt capacitance on the sending end of the π -model of the line that connects buses 1 and 2 is modified accordingly, to account for the shunt capacitor. For this particular test case, it is worth noting that ADMM exhibits oscillations and fails to converge to a solution (see Part I, Fig.9-12).

The results for this specific test-case, for the voltage magnitudes and the active and reactive power of the buses, are shown in Fig. 10. It is worth observing that the proposed algorithm converges to a solution within a few tens of

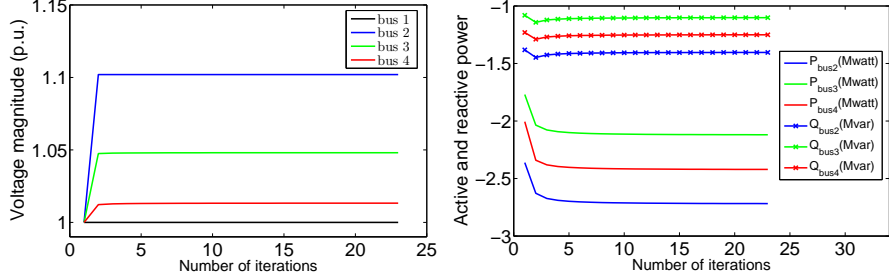


Fig. 10: Evolution of the active and reactive power, as well as the voltages of the buses when a shunt capacitor is connected to bus 2.

iterations; which is contrary to the ADMM-based solution of the OPF problem.

2.5. Performance Evaluation of the Proposed Algorithm under Different Initial Conditions of the Network State

Finally, we investigate the performances of the proposed algorithm under different initial conditions of the network state variables. In order to do so, we initialize the magnitude of the control variables $\bar{E}_{\ell+}^0, \bar{E}_{\ell-}^0, V_b^0$ in Algorithm 1 in the range $[0.9, 1.1]$ and their angle in the range $[-\pi/6, \pi/6]$, totaling 121 different cases. For each combination, we solve the centralized OPF problem for the same network adopted in Part I (Fig. 3). In all the cases the algorithm converges to the same solution within a few tens of iterations. In Table 3, the mean value of the number of iterations, as well as the 95-th percentile are shown. For the sake of brevity, we show in Fig. 11-12 the convergence results for the voltage, as well as for the current flows and the active and reactive power profiles for the two extreme cases, specifically when the voltage magnitude is set to 0.9 (1.1) and the voltage angle is set to $-\pi/6$ ($\pi/6$).

Table 3: Number of iterations for the solution of the OPF problem (Algorithm 1)

	Mean number of iterations	95-th Percentile
Algorithm 1	18.21	46.45

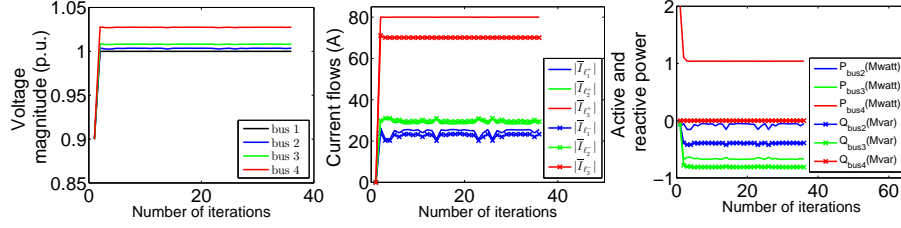


Fig. 11: Evolution of the magnitude of network voltages, line current flows and active and reactive power of the controllable devices when the initial voltage magnitudes are set to 0.9 and the voltage angles to $-\pi/6$.

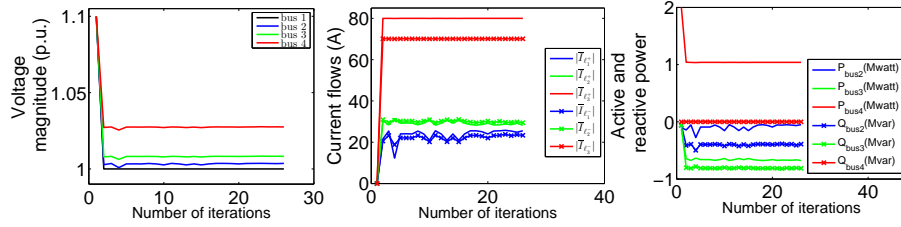


Fig. 12: Evolution of the magnitude of network voltages, line current flows and active and reactive power of the controllable devices when the initial voltage magnitudes are set to 1.1 and the voltage angles to $\pi/6$.

285 3. Performance Evaluation of the Proposed Distributed Asynchronous OPF Algorithm

For the sake of completeness, in this section, we assess the performance of the proposed algorithm with respect to a realistic grid represented by a modified IEEE 13-node test feeder ([19]). The modifications are (i) balanced lines, (ii)
290 inclusion of secondary substations where voltage independent PQ-injections are placed, and (iii) lines ten times longer. We use this benchmark to assess the behavior of the proposed distributed asynchronous OPF algorithm. Also, we compare the solution and convergence of the distributed version of the algorithm to the centralized one.

295 We consider a test case where each network bus, apart from the slack bus, has a load and a generator connected to it. The demand in the network is assumed to be non-controllable, whereas the generators are assumed to be distributed

Table 4: Capability limits and values of loads and generation for the evaluation of Algorithm

2

Bus	$S_{g_{max}}$ (MVA)	$P_c(MW)/$ $Q_c(Mvar)$	Bus	$S_{g_{max}}$ (MVA)	$P_c(MW)/$ $Q_c(Mvar)$
2	0.0437	0.0025 / 0.0011	8	0.0347	0.0031 / 0.0014
3	0.0480	0.0029 / 0.0012	9	0.0403	0.0031 / 0.0013
4	0.0506	0.0032 / 0.0013	10	0.0373	0.0031 / 0.0013
5	0.0367	0.0029 / 0.0012	11	0.0482	0.0024 / 0.0010
6	0.0443	0.0029 / 0.0012	12	0.0399	0.0030 / 0.0013
7	0.0426	0.0025 / 0.0010	13	0.0436	0.0029 / 0.0012

solar panels with typical PV-type capability constraints. For this test case, the capability limits and the values of loads and generation are shown in Table 4.

300 We solve the OPF problem in (8)-(13) using Algorithm 1, as well as the asynchronous implementation of Algorithm 2. The results are shown in Fig. 13-15. For the sake of brevity, we plot only the evolution of the magnitudes of the minimum voltage, the maximum voltage and the median value of the voltage. We plot also the evolution of the minimum, maximum and mean values of the

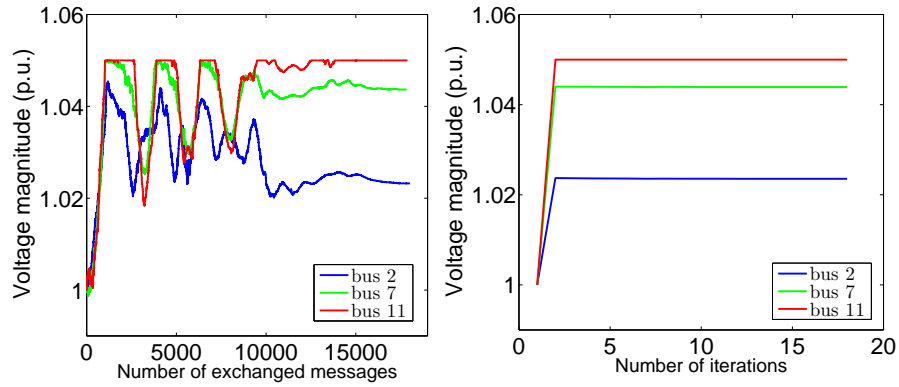


Fig. 13: Evolution of the voltage magnitude for the distributed asynchronous algorithm as a function of the number of messages exchanged (left) and for Algorithm 1 as a function of the number of iterations (right).

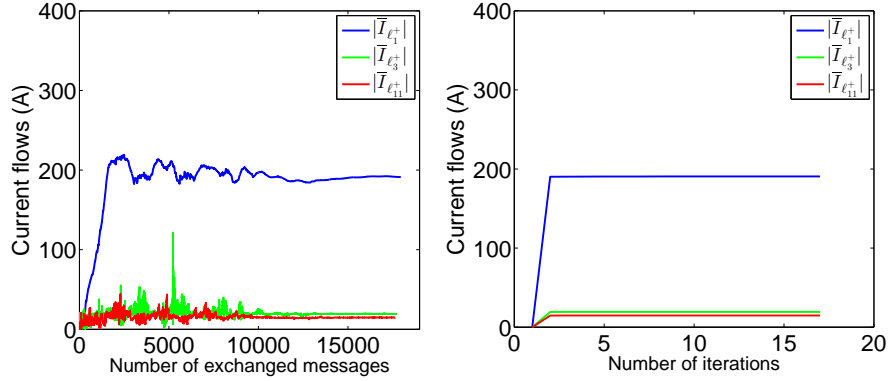


Fig. 14: Evolution of the current flows for the distributed asynchronous algorithm as a function of the number of messages exchanged (left) and for Algorithm 1 as a function of the number of iterations (right).

305 current flows on the receiving-end of the line and the evolution of the active and reactive powers. It is worth observing that Algorithm 1 converges to the optimal solution within a few iterations and also that the distributed asynchronous implementation of Algorithm 1 converges to the same solution as its centralized counterpart.

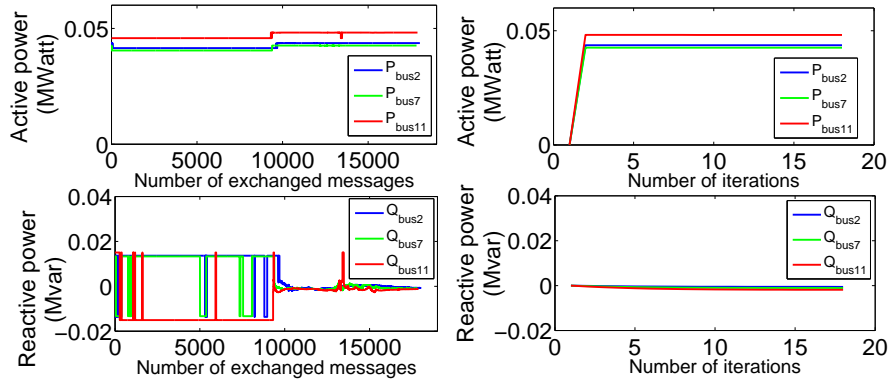


Fig. 15: Evolution of the active and reactive power for the distributed asynchronous algorithm as a function of the number of messages exchanged (left) and for Algorithm 1 as a function of the number of iterations (right).

310 4. Conclusion

To overcome the limitations identified in Part I, we have proposed algorithms for the solution of the AC non-convex OPF problem in radial networks that are proven to converge to a local minimum. These algorithms use an augmented Lagrangian approach and rely on the method of multipliers for the OPF solution. The two algorithms solve the centralized and decentralized (asynchronous) 315 formulation of the targeted OPF. We have shown the robustness of the centralized version with respect to the following elements: (i) various line lengths, (ii) various network-rated voltage values and (ii) different network operating points (cases where the BFM convexification leads to an incorrect solution), (iii) the 320 presence of shunt capacitors in the grid (where ADMM failed to converge to a solution) and (iv) different initial conditions of the electrical network state. Finally, we have verified the equivalence of the two proposed algorithms for the case of the IEEE 13-node test distribution feeder where realistic operating conditions have been considered.

325 References

- [1] M. Farivar, S. H. Low, Branch flow model: Relaxations and convexification - part I, IEEE Trans. on Power Systems 28 (3) (2013) 2554–2564.
- [2] M. Farivar, S. Low, Branch flow model: Relaxations and convexification - part II, IEEE Trans. on Power Systems 28 (3) (2013) 2565–2572. doi: 10.1109/TPWRS.2013.2255318. 330
- [3] A. X. Sun, D. T. Phan, S. Ghosh, Fully decentralized AC optimal power flow algorithms, in: Power and Energy Society General Meeting (PES), IEEE, 2013, pp. 1–5.
- [4] T. Erseghe, Distributed optimal power flow using ADMM, IEEE Trans. on Power Systems 29 (5) (2014) 2370–2380. doi:10.1109/TPWRS.2014. 335 2306495.

- [5] D. P. Bertsekas, Nonlinear Programming, 2nd Edition, Athena Scientific, 1999.
- [6] M. J. Powell, Algorithms for nonlinear constraints that use lagrangian func-
 340 tions, *Mathematical programming* 14 (1) (1978) 224–248.
- [7] M. R. Hestenes, Multiplier and gradient methods, *Journal of optimization theory and applications* 4 (5) (1969) 303–320.
- [8] S. Bolognani, R. Carli, G. Cavraro, S. Zampieri, A distributed control strategy for optimal reactive power flow with power constraints, in: 52nd
 345 Annual Conference on Decision and Control (CDC), IEEE, 2013, pp. 4644–4649.
- [9] S. Bolognani, R. Carli, G. Cavraro, S. Zampieri, A distributed control strategy for optimal reactive power flow with power and voltage constraints, in: IEEE International Conference on Smart Grid Communications (Smart-
 350 GridComm), 2013, pp. 115–120. doi:10.1109/SmartGridComm.2013.6687943.
- [10] E. Dall’Anese, H. Zhu, G. B. Giannakis, Distributed optimal power flow for smart microgrids, *IEEE Trans. on Smart Grid* 4 (3) (2013) 1464–1475.
- [11] B. Zhang, A. Lam, A. Dominguez-Garcia, D. Tse, An optimal and distributed method for voltage regulation in power distribution systems, IEEE
 355 Trans. on Power Systems PP (99) (2014) 1–13. doi:10.1109/TPWRS.2014.2347281.
- [12] M. Kraning, E. Chu, J. Lavaei, S. Boyd, Dynamic network energy management via proximal message passing, *Foundations and Trends in Optimiza-
 360 tion* 1 (2) (2013) 70–122.
- [13] P. Sulc, S. Backhaus, M. Chertkov, Optimal distributed control of reactive power via the alternating direction method of multipliers, *IEEE Trans. on Energy Conversion* 29 (4) (2014) 968–977. doi:10.1109/TEC.2014.2363196.

- 365 [14] Q. Peng, S. H. Low, Distributed algorithm for optimal power flow on a radial network, arXiv preprint arXiv:1404.0700.
- [15] D. P. Palomar, M. Chiang, A tutorial on decomposition methods for network utility maximization, *IEEE Journal on Selected Areas in Communications* 24 (8) (2006) 1439–1451.
- 370 [16] S. Boyd, N. Parikh, E. Chu, B. Peleato, J. Eckstein, Distributed optimization and statistical learning via the alternating direction method of multipliers, *Foundations and Trends® in Machine Learning* 3 (1) (2011) 1–122.
- [17] D. Bertsekas, *Constrained Optimization and Lagrange Multiplier Methods*, 375 *Athena scientific series in optimization and neural computation*, Athena Scientific, 1996.
URL <http://books.google.ch/books?id=-UQZAQAIAAJ>
- [18] A. Geoffrion, Generalized benders decomposition, *Journal of Optimization Theory and Applications* 10 (4) (1972) 237–260. doi:10.1007/BF00934810.
380 URL <http://dx.doi.org/10.1007/BF00934810>
- [19] W. Kersting, Radial distribution test feeders, in: *Power Engineering Society Winter Meeting, 2001. IEEE, Vol. 2, 2001*, pp. 908–912 vol.2. doi:10.1109/PESW.2001.916993.